Research Square

Preprints are preliminary reports that have not undergone peer review.
They should not be considered conclusive, used to inform clinical practice,
or referenced by the media as validated information.

High expression of IGFBP5 in cancer-associated fibroblasts facilitated IGF-2 secretion to promote the metastasis of esophageal squamous cell carcinoma

Hongfang Zhang

zhanghongfang8633@163.com

Hangzhou Cancer hospital

Jing Yue

shuilian wu

zhifeng tian

Rongjing Zhou

tingting zhang

yiping xu

jiajia jin

ruoqi wang

liqing qiu

Mingfeng Jiang

Hangzhou Cancer Hospital

bing xia

Article

Keywords: Esophageal squamous cell carcinoma, Cancer-associated fibroblasts, Metastasis, IGFBP5, IGF-2, Inflammatory Phenotype, Immunosuppressive microenvironment

Posted Date: November 19th, 2026

DOI: https://doi.org/10.21203/rs.3.rs-11462186/v1

License: This work is licensed under a Creative Commons Attribution 4.0 International License.
Read Full License

Additional Declarations: There is **NO** conflict of interest to disclose.

High expression of IGFBP5 in cancer-associated fibroblasts facilitated IGF-2 secretion to promote the metastasis of esophageal squamous cell carcinoma

Jing Yue[1#], Shuilian Wu[2#], Zhifeng Tian[3,4#], Rongjing Zhou[5#], Tingting Zhang[5], Yiping Xu[5], Jiajia Jin[6,7], Ruoqi Wang[1], Liqing Qiu[1], Mingfeng Jiang[2], Bing Xia[8], Hongfang Zhang[1*]

[1]Hangzhou Cancer Institution, Hangzhou Cancer Hospital, Hangzhou, China, 310002
[2]Department of Clinical Laboratory, Hangzhou Cancer Hospital, Hangzhou, China, 310002
[3]Department of Oncology Center, The Fifth Affiliated Hospital of Wenzhou Medical University, Lishui, China, 323000
[4]Lishui Central Hospital, Lishui 323000, China
[5]Department of pathology, Hangzhou Cancer Hospital, Hangzhou, China, 310002
[6]Zhejiang Chinese Medical University, Hangzhou, China, 310053
[7]The First People's Hospital of Yuhang District, Hangzhou, China, 311100
[8]Department of thoracic oncology, Hangzhou Cancer Hospital, Hangzhou, China, 310002

[#]These authors contributed equally to this manuscript.
*To whom correspondence should be addressed: Hangzhou Cancer Institution, Hangzhou Cancer Hospital, Hangzhou, China, 310002. Tel./fax: +86 571 56006035; E-mail address:zhanghongfang8633@163.com;
The authors declare that they have no competing interests.

Abstract

Esophageal squamous cell carcinoma (ESCC) is a highly aggressive malignancy. Cancer-associated fibroblasts (CAFs) as one major component of tumor microenvironment (TME) have close association with tumor progression. However, the mechanisms by which CAFs promoted ESCC metastasis have remained unclear. By injection of ESCC cells alone or in combination of CAFs into mice, we examined whether CAFs influenced the metastasis of ESCC cells in vivo. By single-cell RNA sequencing (scRNA-seq) and high throughput screening of 157 kinase inhibitors, we discovered the critical subtype of CAFs influencing ESCC metastasis. In vitro, we found CAFs promoted the invasion of ESCC cells by inducing epithelial-mesenchymal transition (EMT) through activating YAP signaling. In vivo, CAFs promoted lymphatic and pulmonary metastasis of ESCC cells. By scRNA-seq and high throughput screening, we revealed the subtype of CAFs with high expression of IGFBP5 secreted IGF-2 to promote ESCC metastasis. Inhibition of IGF-2 secretion reduced the proliferation and activation of CAFs through decreasing the expressions of Cyclin D1 and TGFβ-1, respectively. In turn, ESCC cells induced inflammatory phenotype of CAFs by increasing CXCL1 expression, which activated cGAS-STING pathway, to establish an immunosuppressive microenvironment. Together, our study highlighted CAFs-sourced IGF2 signaling as an attractive target of inhibiting ESCC metastasis.

Key Words: Esophageal squamous cell carcinoma; Cancer-associated fibroblasts; Metastasis; IGFBP5; IGF-2; Inflammatory Phenotype; Immunosuppressive microenvironment;

Background

Esophageal squamous cell carcinoma (ESCC) is one major pathological type of esophageal carcinoma (EC). Especially, in Asian countries, ESCC accounted for approximately 90 % of EC cases [1]. Since the early symptoms are not obvious, about 70 %-80 % ESCC patients are diagnosed at middle or advanced stage, with a five-year survival rate of 15 % [2]. Even for those patients with resectable ESCC, the five-year survival rate is only 20 %-30 %. One main cause of poor prognosis is the highly invasive ability of ESCC which easily leads to the metastasis of tumors to lymph nodes and even distant organs such as lung and liver [3, 4]. As reported, the percentage of tumor metastasis is 50 % in primary ESCC patients [5]. Even in those patients treated with surgery, the incidence of tumor metastasis is still as high as 30 %-70 % [6, 7]. Several studies demonstrated that the sensitivity of metastatic tumors to original treatment schedule is significantly lower than that of primary tumors, suggesting that metastatic tumors is highly resistant to chemotherapy and radiotherapy [8, 9]. Although immunotherapy such as immune checkpoint inhibitors (ICIs) is prescribed as a first-line therapy for metastatic ESCC patients, only 20 % of patients benefit [4]. Effective choices for metastatic ESCC patients is severely lack. Therefore, the metastasis is a lethal event for most of ESCC patients.

Tumor metastasis is very complex and experiences multi-steps. Tumor cells need to acquire enough ability to degrade extracellular matrix (ECM), invade into and out blood vessels and grow into metastatic colonies in other organs [10]. Factually, tumor cells grow not in isolation but severely rely on their microenvironment. Therefore, their metastasis was fine-tuned by the microenvironment [11]. CAFs, which are one major component of the tumor microenvironment (TME), were discovered to be closely associated with tumor initiation and progression [12]. In comparison with tumor cells, CAFs have more survival advantages following chemoradiotherapy since they have strong DNA repair and anti-oxidant ability [13]. So, they may support those surviving tumor cells metastasize after chemoradiotherapy. More importantly, CAFs lead collective invasion of tumor cells with epithelial phenotype by remodeling the ECM [14]. CAFs generate a track through the matrix through which tumor cells invade behind fibroblasts. Tumor cells themselves have no enough ability to achieve a collective invasion due to lack in both force-mediated and protease-mediated matrix remodeling. In CAFs, the matrix remodeling pathways are significantly activated, while they are not essential for invasive tumor cells, suggesting that CAFs are the leading cells of tumor invasion. Furthermore, the tumor cells which succeeded in metastasis must escape from immune surveillance [15]. Therefore, tumor metastasis relied on an establishment of immunosuppressive microenvironment. CAFs have the ability of establishing an immunosuppressive microenvironment via several mechanisms to help metastatic tumor cells escape from immune surveillance [16].

In ESCC, CAFs were reported to mediate the resistance of tumor cells to chemoradiotherapy via several mechanisms [17]. However, the association of CAFs and tumor metastasis was less studied in ESCC. In our study, we explored the effect of CAFs on the metastasis of ESCC to lymph nodes and even distant organs and

involved mechanisms. By single cell RNA-sequencing (scRNA-seq) as well as high throughput screening, we revealed the subtype of CAFs with high expression of IGFBP5 secreted IGF-2 to promote ESCC metastasis to lymph nodes and lung through activation of YAP signaling. Down-regulation of IGF-2 also inhibited the proliferation and activation of CAFs by down-regulating Cyclin D1 and TGFβ-1, respectively. In turn, ESCC cells reshaped CAFs to establish an immunosuppressive microenvironment by up-regulating CXCL1 to activate cGAS-sting pathway during their interaction. These findings in our study may aid in deeper understanding of the association of CAFs and tumor metastasis and shed novel lights into the development of anti-ESCC metastasis strategies.

Materials and Methods

Isolation of primary stromal fibroblasts

To isolate stromal CAFs, tumor tissues were obtained with the permission of patients with ESCC who had not been treated with any preoperative chemoradiotherapy before esophagectomy. The use of tumor tissues was in accordance with the guidelines of the Committees for Ethical Review of Research at Hangzhou Cancer Hospital (Hangzhou, China). The isolation of CAFs in ESCC was accomplished according to the method described in our previous study (8). CAFs-1 and CAFs-2 were isolated from two ESCC patients, respectively.

Culture of esophageal squamous cell carcinoma cells, normal esophageal epithelial cells Het-1A and CAFs

The normal esophageal epithelial cells Het-1A were from American Type Culture Collection. ESCC cells including KYSE-150, Eca109, TE-10 and KYSE-30 were purchased from Shanghai Institutes for Biological Sciences, Chinese Academy of Sciences (Shanghai, China). ESCC cells and CAFs were cultured in RPMI-1640 medium (Jiangsu KeyGEN Bio TECH Corp., Ltd, Nanjing, China) with 10 % fetal bovine serum (Corning, NY, USA). Het-1A cell lines were cultured in DMEM medium (Jiangsu KeyGEN Bio TECH Corp., Ltd, Nanjing, China) with 10 % fetal bovine serum (Corning, NY, USA).

Preparation of the conditioned medium

CAFs or ESCC cells were seeded into 75-cm^2 culture flask. Forty-eight hours later, when the cells were grown at approximately 80% confluence, the culture medium was collected and centrifuged at 3,000 rpm at 4℃ for 30 minutes. The supernatant was collected as conditioned medium and kept at ultra-low temperature freezer until use. The conditioned medium from CAFs or ESCC cells was defined as CAFs medium or KYSE-150/Eca109 medium. Normal medium was fresh RPMI1640 medium with 10% FBS.

Antibodies, agents and animals

Antibodies against Ly-6G (E6Z1T, 87048), CD206 (E6T5J, 24595) , α-SMA (1A4, 48938), TGF-β1 (56E4, 3709), Ki-67 (D3B5, 12202), PD-L1 (E1L3N, 13684), TBK1 (D1B4, 3504), Phospho-TBK1 (Ser172) (D52C2, 5483), IRF-3 (D6I4C, 11904) were purchased from Cell Signaling Technology (Beverly, MA, USA). Antibodies against IGF-2 (JJ092-3, ET1701-88), CXCL1 (PSH07-53, HA722841), IL1β (JJ087-3,

ET1701-39), IL-8(PSH10-97, HA723264), Phospho-IRF3 (S386)(SU03-28, ET1608-22), MPO(A1F2, ET1901-19), YAP (SU33-06, ET1608-30) was purchased from Hangzhou Huaan Biotechnology Co., Ltd (Hangzhou, China). The antibody against IGFBP5 (PB0749) was purchased from Boster Biological Technology Co. Ltd. (Wuhan, China).The antibody against pan-CK(B32114R) was purchased from Haoke Biotechnology Co., Ltd (Hangzhou, China). The antibody against GAPDH was purchased from Absin Bioscience (Shanghai, China). HRP AffiniPure Goat Anti-Rabbit IgG was purchased from Hangzhou Fude Biological Technology Co., Ltd (Hangzhou, China). BCA Protein Assay Kit was purchased from Jiangsu KeyGEN Bio TECH Corp., Ltd (Nanjing, China). RNA-Quick Purification Kit was purchased from Shanghai Yishan Biotechnology Co., Ltd (Shanghai, China).. H-151(HY-112693), PMA(HY-18739), IL-4(HY-P70445), IL-13(HY-P70568) were purchased from MedChemExpress (NJ, USA). EndoFectin™ RNAi and EndoFectin™ Max transfection reagent were purchased from GeneCopoeia, Inc.(MD, USA). DAPI (D9542) was purchased from Sigma-Aldrich (MO, USA). CCK-8 kit was purchased from UELandy (Suzhou, China). Chemically synthesized siRNAs, the CXCL1 overexpression plasmid, and shIGF-2 lentiviral vectors were constructed and provided by GenePharma Co., Ltd. (Shanghai, China).

4-week-old female BALB/c nude mice were purchased from Shanghai SLAC Laboratory Animal Co, Ltd. (Shanghai, China) and maintained under standard conditions in Experimental Animal Center in Zhejiang Chinese Medicine University (Zhejiang, China). All of animal protocols in our study were in accordance with the institutional animal welfare guidelines of Zhejiang Chinese Medicine University.

Transfection

The cells were cultured until adherent growth and then transfected with the mixture of EndoFectin™ RNAi and siRNA against indicated genes or EndoFectin™ Max and CXCL1-overexpression plasmids. 6 h later, the medium was replaced with RPMI-1640 medium. After 48 h, the proteins and RNAs were extracted from the cells and examined by western blotting and qRT-PCR analysis, respectively. Scrambled siRNA were used as a negative control. The sequences of siRNA against target genes were shown in Supplementary Table S1.

Lentivirus preparation and infection

The IGF-2 shRNA was cloned into the lentiviral expression vector LV3-pGLV-h1-GFP-puro and scrambled shRNA cloned into LV3-pGLV-h1 vector as negative control. CAFs were transfected with lentivirus vectors containing IGF-2 shRNA or scrambled shRNA as negative control. 24 h later, the culture medium was replaced with fresh medium and the cells were cultured for another 72 h. The transfected cells were cultured in the presence of 1 μg/ml puromycin. After 14 days' culture, the surviving cells were collected and tested for IGF-2 expression using qRT-PCR analysis.

qRT-PCR analysis

Total RNA was extracted from cells using RNA-Quick Purification Kit (Yishan Biotechnology, Shanghai, China) following the manufacturer's instructions. Reverse transcription was performed with PrimeScript RT Master Mix(Takara, Kusatsu, Japan)

following the manufacturer's instructions. Quantitative RT-PCR (qRT-PCR) was conducted using TB green (Takara, Kusatsu, Japan) according to the manufacturer's instructions. The PCR primers used in our study were synthesized by Sangon Biotech Co., Ltd (Shanghai, China) and shown in Supplementary Tables S2.

CCK8 assay

The cells were seeded into 96-wells plate and their sensitivity to kinase inhibitors was detected using CCK8 assay. After adherent growth, the cells were cultured in the medium containing indicated drugs. 48 h later, the CCK8 reaction solution was added into each well and the cells were cultured for another 2 h. Then, the absorbance of cells was examined at 450 nm using a microplate spectrophotometer (Molecular devices spectraMax i3, San Francisco, CA, USA). The cell viability was expressed as a percentage of kinase inhibitors-treated cells relative to that of untreated cells.

Single-cell RNA sequencing (scRNA-seq)

CAFs were collected and washed twice with PBS and prepared into single-cell suspensions. Then, they were exposed to scRNA-seq (Singleron Biotechnology Co., Ltd., Nanjing, China). Automated library construction was performed using Singleron Matrix NEO®. The bioinformatics tool of CeleScope® and SynEcoSys® database were used for data analysis. 7 distinct clusters were identified in dimension-reduction (UMAP) analysis, and the differentially expressed genes of each cluster were labeled.

High-throughput screening of cytokines/chemokines inhibitors

The library of 157 kinase inhibitors was purchased from Shanghai Topscience Co., Ltd (Shanghai, China) (Supplementary Table S3). CAFs were seeded into 96-wells plate. After adherent growth, the medium was replaced with fresh medium in which the combination of 10 μM kinase inhibitors was added. 24 h later, the viability of CAFs cells was detected using CCK8 assay. After primary screening, the TOP ten kinase inhibitors which inhibited the viability of CAFs were selected for second screening. During this process, CAFs as well as normal esophageal epithelial cell Het-1A and ESCC cells including KYSE-150 and Eca109 were used to test the effect of kinase inhibitors at a dose concentration of 2.5, 5, 7.5, 10 μM, respectively, according to the procedures in the primary screening. We finally chose the kinase inhibitor which can specifically inhibit CAFs but not esophageal cancer cells and Het-1A for further studies.

RNA sequencing (RNA-seq)

The effect of CAFs on the genes signature of ESCC cells as well as the effect of IGF-2 down-regulation on CAFs was detected using RNA-seq. Briefly, the RNA samples were extracted and sent to Novogene (Beijing, China) for bulk RNA-seq according to the procedures. The threshold of screening differentially expressed genes was p-value<=0.05, |log2FoldChange|>=1.0. The significantly enriched pathways were identified with KEGG analysis (padj<0.05).

Immunohistochemical (IHC) analysis

IHC staining of interested proteins was performed on paraffin-embedded sections of tumor tissues, lymph nodes or pulmonary nodules. Briefly, sections of 4 μm thick were deparaffinated and rehydrated trough a series of graded alcohols. Endogenous

peroxidase activity was quenched with 3% (v/v) H2O2 for 20 min. Nonspecific binding was avoided by immersing sections into 3% BSA in PBS for 30 min at room temperature. Then, the sections were incubated with the primary antibody and HPR-conjugated secondary antibody. The slides were scored by a pathologist and two experienced researchers independently.

Immunofluorescence (IF) analysis

The expression and cellular distribution of YAP in esophageal cancer cells which were cultured in normal medium or CAFs medium were detected by immunofluorescence analysis. The cells were incubated with YAP antibody (ET1608-30, Hua-bio, Hangzhou, China) and then Alexa Fluor 488-conjugated secondary antibody (A11019, Thermo Fisher Scientific Inc., MA, USA). DAPI was used to label the nucleus. Immunofluorescence images were collected with a Live-cell imaging system (FV10i-LIV, Olympus, Tokyo, Japan).

Western blotting

The expressions levels of proteins were detected using western blotting. Briefly, cells after indicated treatments were harvested by trypsin-EDTA exposure and washed twice with ice-cold PBS before adding into protein extraction buffer. Equal amount of proteins was fractionated on SDS-PAGE gel and transferred to polyvinylidence difluoride membranes. The membranes were incubated with indicated primary and secondary antibodies. Proteins were ultimately visualized by enhanced chemiluminescence and autoradiography (Fude Biological Technology, Hangzhou, China).

Transwell assays

Approximately 100 μl of matrigel diluted with serum-free RPMI-1640 medium at a ratio of 1:40 was pre-plated in the upper layer of the chamber. 6 h later, CAFs or ESCC cells which had underwent a 12 h starvation period in serum-free medium were seeded into the upper chamber. And the complete RPMI-1640 medium with 10 % FBS was added into the lower chamber. 48 h later, the cells were fixed with 4 % paraformaldehyde for 10 min and then stained with 0.1 % crystal violet for another 10 min. The invaded cells were observed using an Olympus microscope and quantitatively analyzed via the Image J software.

Detection of glucose uptake and lactate secretion

CAFs were transfected with IGF-2 siRNA or scrambled siRNA. 24 h later, the cells were cultured in sugar-free medium for 24 h of starvation before culture in the medium containing equal amount of glucose for another 48 h. The medium was then centrifuged at 7000 rpm for 5 min. After cell counting, the glucose uptake and lactate secretion in the supernatant of 105 cells in different groups were detected with glucose assay kit (BB-47302-1000T, Bestbio, Shanghai, China) and lactic acid determination kit (KGT023, Jiangsu KeyGen Bio TECH Croup., Ltd., Nanjing, China), respectively, following the manufacturer's instructions.

Isolation of neutrophils and Detection of Neutrophil Extracellular Traps, NETs

Peripheral blood was provided by healthy volunteers and kept in heparinized tubes. Then, the blood was mixed with Histopaque-1077 (10771, Sigma-Aldrich, USA) according to the manufactures' instructions and then centrifuged to obtain the mix of

neutrophils and Red blood cells. Using Red blood cell lysis buffer to remove red blood cells, the neutrophils were washed with PBS two times and cultured in RPMI-1640 medium supplemented with 10 % FBS.

Neutrophils were seeded on Poly-L-lysine-coated slide and cultured under different conditions including RPMI-1640 medium, CAFs medium and RPMI-1640 medium with 400 nM PMA. 6 h later, the cells were fixed with 4% paraformaldehyde, permeabilized with triton X-100 and blocked with 5 % bovine serum albumin. Then, the cells were incubated with anti-MOP antibody and FITC-conjugated secondary antibody. The cell nucleus was visualized by DAPI staining. NETs were observed using confocal Live-cell imaging system (FV10i-LIV, Olympus, Tokyo, Japan).

M2 macrophages polarization

THP-1 cells were cultured in the RPMI-1640 medium with 10 % FBS and 0.05 mM mercaptoethanol and seeded into 6-wells plate at a density of 3×105 cells/well and exposed to 100 ng/mL PMA. 24 h later, the cells showed adherent growth with pseudopods and were defined as M0 macrophages. To explore the effect of CAFs on M0 macrophages, we cultured M0 macrophages in CAFs medium in which CXCL1 was overexpressed or not. After 72 h culture, the cells were collected to extract proteins. Then, WB analysis was performed to detect the expression level of CD206, a marker of M2 macrophages in the cells.

M2 macrophages recruitment

THP-1 cells were cultured in the RPMI-1640 medium with 10 % FBS and 0.05 mM mercaptoethanol and exposed to 100 ng/mL PMA. 24 h later, the cells were washed twice with PBS and cultured in complete RPMI-1640 medium for 6 h. Then the medium was supplemented with IL-4 (20ng/mL) and IL-13 (20ng/mL) and the cells were stimulated for another 48 h, allowing the transformation of M2 macrophages. And the recruitment of M2 macrophages by CAFs-secreted CXCL1 was detected using transwell assay. Briefly, M2 macrophages were seeded into the upper layer of the chamber. 24 h later, the cells were cultured in serum-free medium and CAFs medium in which CXCL1 was overexpressed was added into the lower chamber. 48 h later, the cells were fixed with 4 % paraformaldehyde for 15 min and then stained with 0.1 % crystal violet for another 10 min. The recruited M2 macrophages were observed using an Olympus microscope and quantitatively analyzed via the Image J software.

Mouse model of lymphatic metastasis and pulmonary metastasis

To establish mouse model of pulmonary metastasis, ESCC cells alone or in combination with CAFs at a ratio of 1:1 was injected into BALB/c nude mice via tail vein. The body weight of mice was monitored every week. After 8 weeks, the mice was executed and dissected to obtain the lung tissues. After fixation with formalin and H&E staining, the number and maximum diameter of pulmonary nodules in each mice were analyzed by a pathologist and two experienced researchers independently.

To establish mouse model of lymphatic metastasis, ESCC cells alone or in combination with CAFs at a ratio of 1:2 were injected into the foot pad of BALB/c nude mice. The body weight of mice was monitored every week. After 8 weeks, the

mice was executed and the tumor tissues in the foot pad as well as ipsilateral popliteal lymph nodes were resected. The tumor tissues were weighted and the ipsilateral popliteal lymph nodes were measured to obtain the maximum diameter (A) and the minimal diameter (B), respectively. And the volume of lymph nodes was obtained using the formula: $V(mm3)= A(mm)\times B(mm)^2/2$. The lymph nodes were also analyzed using IHC staining to evaluate the percentage of metastatic cancer cells.

Statistical analysis

All of the experiments were independently repeated in triplicate and the data were shown as means ± SD. GraphPad Prism 9.0 was used for statistical analysis. Two-tailed Student's t-tests were employed to evaluate differences between two groups and one-way analysis of variance (ANOVA) was used for comparisons among multiple groups with just a single factor while two way ANOVA was used among multiple groups with two factors.

Results

CAFs initiated the EMT phenotype of ESCC cells through activating YAP signaling pathway

Since ESCC is a highly aggressive malignance, our study aimed to detect the effect of CAFs, one major component of the TME, on the metastasis of ESCC cells. We found CAFs significantly promoted the invasive ability of several ESCC cells including KYSE-30, Eca109, KYSE-150 and TE-10 (Figure.1A). We then adopted RNA-seq to analyze the gene signature of esophageal cancer cells which were co-cultured with CAFs. As described above, epithelial to mesenchymal transition (EMT) is an important mechanism for cancer cells to acquire the invasive ability. When esophageal cancer cells were co-cultured with CAFs, the epithelial markers were significantly down-regulated while the mesenchymal markers as well as EMT-associated transcription factors were all significantly up-regulated as shown in Figure.1B and1C . Furthermore, the ability of degrading ECM in esophageal cancer cells was also increased by highly expressing MMPs (Figure.1C). KEGG analysis showed that Hippo signaling pathway was significantly changed in esophageal cancer cells which were co-cultured with CAFs (Figure.1D). When Hippo signaling pathway was inactivated, YAP as a core component of this pathway is dephosphorylated and translocated from the cytoplasm into the nucleus to initiate the transcription of target genes such as AREG and SERPINE1 to induce EMT to promote tumor metastasis. In our study, we found YAP was up-regulated and translocated from the cytoplasm into the nucleus in esophageal cancer cells which were co-cultured with CAFs (Figure.1E). Furthermore, we found the expressions of AREG and SERPINE1 both of which are reported to promote tumor metastasis were increased in esophageal cancer cells which were co-cultured with CAFs (Figure.1F). When YAP was down-regulated by transfection with its siRNA in esophageal cancer cells before co-culture with CAFs, the invasive ability of cancer cells was significantly attenuated (Figure.1G,1H). These results suggested that CAFs enhanced the invasive ability of esophageal cancer cells by inducing EMT possibly through activating YAP signaling.

CAFs promoted lymphatic and pulmonary metastasis of ESCC cells in vivo

Furthermore, we established two metastatic models in nude mice to discover the role

of CAFs in ESCC metastasis in vivo. By injection of tumor cells alone or in combination of CAFs into foot pad of the mice, we examined whether CAFs could influence lymphatic metastasis of ESCC cells in vivo. Furthermore, by tail vein injection of tumor cells alone or in combination of CAFs, we examined the effect of CAFs on distant metastasis of ESCC cells such as lung metastasis. As shown in Figure.2A and 2B, we found the tumors in situ implanted with the combination of CAFs and tumor cells showed a larger volume compared with that implanted with only tumor cells. More importantly, the lymph nodes of mice were significantly enlarged in the group implanted with the combination of CAFs and tumor cells, suggesting that ESCC cells may invade into the lymph nodes. By HE and IHC staining, we confirmed that CAFs induced the lymphatic metastasis of ESCC cells in nude mice while lymphatic metastasis did not occur in the xenograft tumors where only ESCC cells but not in combination of CAFs were implanted (Figure.2C, 2D). These results suggested that CAFs not only accelerated tumor growth in situ but also aid in their spread, leading to lymphatic metastasis. Furthermore, consistent with the in vitro results, we found YAP was also up-regulated in the tumors in situ where CAFs were implanted(Figure.S1). In tail vein injection mouse model, we found that the number of pulmonary nodules in the mice implanted with the complex of CAFs and tumor cells was higher than that in the group implanted with only tumor cells (Figure.2E, 2F), suggesting that CAFs increased pulmonary metastasis of ESCC cells. We then analyzed the composition of immune microenvironment of xenograft tumors. As shown in Figure.2G, we found tumor cells were surrounded by CAFs in tumors (in situ). Furthermore, we found CAFs were located in the leading edge of invasive tumor tissues, suggesting that CAFs may lead the invasiveness of tumor cells (Figure.2G). Meanwhile, there were a large number of neutrophils which are evidenced to support ESCC metastasis in the invasive tumor tissues; M2 type macrophages as a main type of immunosuppressive immune cells, were also found to be significantly increased in the invasive tumor tissues(Figure.2H). Therefore, the reshape of tumor microenvironment may help ESCC cells acquire the invasive ability when CAFs were implanted into the xenograft tumors.

IGFBP5^{high} CAFs promoted the invasive ability of ESCC cells by secreting IGF-2 signaling

We then explored how CAFs promoted the malignant phenotype of ESCC cells. By scRNA-seq, we detected the heterogeneity of ESCC CAFs. We found there were several subtypes such as IGFBP5 highly expressing CAFs (IGFBP5^{high} CAFs) among ESCC CAFs (Figure.3A). GO analysis suggested that IGFBP5^{high} CAFs have several ECM remodeling-associated functions, suggesting that this population may be involved in ESCC metastasis (Figure.3B). Therefore, we examined the expression of IGFBP5 in CAFs as well as in ESCC cells and normal esophageal epithelial cells Het-1A. As shown in Figure.3C, we found IGFBP5 was mainly expressed in CAFs compared with ESCC cells and Het-1A. When IGFBP5 was down-regulated, the invasive ability of CAFs was attenuated(Figure.3D, 3E). Since IGFBP5 functions as a critical regulator of IGF-1/2 expression, we examined the expressions of IGF-1 and IGF-2 in CAFs, ESCC cells and Het-1A. As shown in Figure.3F, IGF-2 was highly

expressed in CAFs compared with IGF-1 in CAFs. When IGFBP5 was down-regulataed, the expression of IGF-2 was significantly decreased(Figure.3G, 3H), suggesting that IGFBP5 functions as a stabilizer of IGF-2 expression.

Furthermore, we found the autocrine and paracrine IGF-2 signaling was activated when CAFs were co-cultured with ESCC cells (Figure.4A-4C). Therefore, we speculated that CAFs-secreted IGF-2 may play a major role in the interaction of CAFs and esophageal cancer cells. When the expression of IGF-2 was decreased by transfection with IGF-2 siRNA (Figure.4D), we found the invasive ability of CAFs were attenuated (Figure.4E). Furthermore, the promoting effect of CAFs on YAP activation was attenuated and the invasive ability of co-cultured esophageal cancer cells was reduced when CAFs were transfected with IGF-2 siRNA (Figure.4F, 4G). We also found the expressions of α-SMA, a marker of CAFs activation was decreased along with the down-regulation of TGFβ-1 which is recognized as a classical inducer of CAFs activation when CAFs were transfected with IGF-2 siRNA (Figure.4H). So, high expression of IGFBP5 in CAFs facilitated the secretion of IGF-2, leading to CAFs activation possibly through activating TGFβ-1 signaling. Meanwhile, the high-throughput screening of 157 kinase inhibitors also showed that inhibition of IGF-2/IGF-1R pathway, significantly suppressed the viability of CAFs; in comparison, inhibition of IGF-2/IGF-1R pathway did not show inhibitory effect on esophageal cancer cells as well as normal epithelial cells HET-1A (Figure.4I, 4J, S2). These results suggested that the IGF-2/IGF-1R signaling may be specially activated in CAFs but not in esophageal cancer cells and in normal epithelial cells.

Inhibition of CAFs-secreted IGF-2 signaling attenuated tumor metastasis in vivo

We then explored whether down-regulation of IGF-2 in CAFs could attenuate the metastasis of esophageal cancer cells in vivo. When cancer cells were mixed with IGF-2^{low} CAFs where IGF-2 was down-regulated (Figure.S3), the tumors in foot pad of mice were significantly smaller than that implanted with the mixture of cancer cells and control CAFs where scrambled shRNA was transfected. Accordingly, the tumors implanted with IGF-2^{low} CAFs had significantly decreased weight compared with that implanted with control CAFs. Furthermore, we found the lymph nodes of mice implanted with the mixture of esophageal cancer cells and control CAFs were enlarged at a higher degree than that implanted with the mixture of esophageal cancer cells and IGF-2^{low} CAFs (Figure.5A). This difference indicated that down-regulation of IGF-2 may attenuate the infiltration of esophageal cancer cells into lymph nodes. To confirm our hypothesis, we detected the expression of pan-CK, a marker of epithelial-derived tumor in the lymph nodes. As shown in Figure.5B, the pan-CK-positive area in lymph nodes of mice implanted with the mixture of esophageal cancer cells and control CAFs was significantly larger than that of mice implanted with the mixture of esophageal cancer cells and IGF-2^{low} CAFs. In the metastatic model established by tail vein injection, we found there were not significant difference in the number of pulmonary nodules between the two groups (Figure.S4). However, we found the maximum diameter of pulmonary nodules was smaller in the group implanted with the mixture of cancer cells and IGF-2^{low} CAFs than that in the group implanted with the mixture of cancer cells and control CAFs

(Figure.5C). We further detected the express of Ki-67, an indicator of cell proliferation, in these two groups. As shown in Figure.5C, the expression of Ki-67 was lower in the group implanted with the mixture of cancer cells and IGF-2^{low} CAFs than that in the group implanted with the mixture of cancer cells and control CAFs. These results suggested that down-regulation of IGF-2 may attenuate the malignant progression of pulmonary nodules. Furthermore, due to IGF-2 down-regulation in CAFs, the number of neutrophils and M2 macrophages were both reduced (Figure.5D), suggesting that attenuation of IGF-2 signaling in CAFs may reshape the tumor microenvironment of ESCC.

The IGF-2 signaling in CAFs regulated Cyclin D1 expression and glycolysis

To perform a systemic analysis on IGF-2 signaling in CAFs, we adopted RNA-seq to detect the gene signature of CAFs where IGF-2 was down-regulated. As shown in Figure.6A, KEGG analysis revealed that cell cycle pathway was significantly enriched in CAFs when IGF-2 was down-regulated. Among the top-changed genes in cell cycle pathway, we found Cyclin D1 was the most significantly changed gene (Figure.6B, 6C). Cyclin D1 serves as a crucial cell cycle regulator and has been identified as a metastatic promoter in several human cancers [18]. We found down-regulation of Cyclin D1 in CAFs induced the cell cycle arrest in G0/G1 phase and therefore reduced cell proliferation (Figure.6D-6F, S5). Down-regulation of Cyclin D1 also attenuated the invasive ability of CAFs (Figure.6G). Furthermore, due to that the invasiveness of CAFs is an energy-consuming process, we detected whether the IGF-2 signaling in CAFs was involved in cell metabolism. Compared with the metabolism of lipid and amino acid, we found the genes involved in glycolysis including the glucose transporter GLUT1, rate-limiting glycolytic enzyme PKM and lactate transporter MCT4 were significantly changed in CAFs where IGF-2 was down-regulated (Figure.6H, 6I). Function studies revealed that both the uptake of glucose and the secretion of lactate were reduced in CAFs where IGF-2 was down-regulated (Figure.6J). These results suggested that down-regulation of IGF-2 inhibited the glycolysis of CAFs. Furthermore, we found that the expression of Cyclin D1 was decreased in CAFs when the glycolysis was inhibited through down-regulation of MCT4 (Figure.6K). Therefore, we speculated that the activation of glycolysis may be the basis of CAFs to promote the progression of ESCC.

ESCC cells transformed CAFs to establish an immunosuppressive microenvironment by up-regulating CXCL1

Since there is a reciprocal interaction of CAFs and cancer cells, we therefore explored the effect of esophageal cancer cells on CAFs during the metastasis. By RNA-seq, we found the co-culture of esophageal cancer cells and CAFs significantly influenced the transcriptome of CAFs. KEGG analysis revealed that cytokine-cytokine receptor was changed most significantly during the interaction of CAFs and ESCC cells (Figure.7A). Several immunosuppressive chemokines such as CXCL1, IL8 and IL1β were among the TOP 10 up-regulated genes in CAFs which were co-cultured with ESCC cells (Figure.7B-7E). Furthermore, PD-L1 which serves as an inducer of $CD8^+$ T cells exhaustion by binding to its receptor PD-1, was significantly up-regulated both in CAFs and in esophageal cancer cells during their interaction (Figure.7F). These

results suggested that the co-cultured of esophageal cancer cells and CAFs may transform CAFs into an inflammatory phenotype to establish an immunosuppressive microenvironment. Since the metastasis of tumors relies on an establishment of immunosuppressive environment, we then explored how the interaction of CAFs and esophageal cancer cells affected the immune microenvironment. Protein-protein interaction analysis showed that CXCL1 may interact with TBK1, a core component of the cGAS-sting signaling pathway which is known as an active modulator of the immune microenvironment (Figure.8A). We therefore examined whether CXCL1 activated the cGAS-sting signaling pathway. As shown in Figure.8B, when CAFs were co-cultured with esophageal cancer cells, the critical components of cGAS-sting pathway was significantly changed. The phosphorylation of TBK1 was significantly increased. Phosphorylated TBK1 then promoted the phosphorylation of IRF3, leading to the transcription of downstream immune regulatory genes. When the expression of CXCL1 was decreased by transfection with its siRNA, the activation of cGAS-sting signaling pathway was significantly attenuated in CAFs which were co-cultured with esophageal cancer cells (Figure.8C). To further confirm the association of cGAS-sting pathway and immune regulation in CAFs, we detected the expressions of PD-L1, IL-8 and IL1β in CAFs in which the cGAS-sting pathway was blocked with H151 before co-culture with esophageal cancer cells. As shown in Figure.8D and 8E, the up-regulation of PD-L1, IL-8 and IL1β was significantly attenuated in CAFs which were pretreated with H151 before co-culture with esophageal cancer cells. Similarly, when CXCL1 was down-regulated in CAFs by transfection with its siRNA before co-culture with esophageal cancer cells, the up-regulation of PD-L1, IL-8 and IL1β was significantly attenuated (Figure.8F). These results suggested that esophageal cancer cells induced inflammatory phenotype of CAFs through up-regulating CXCL1, which then activated cGAS-sting pathway to establish an immunosuppressive environment by highly expressing PD-L1, IL-8 and IL1β. Together, the schematic diagram of CAFs in ESCC metastasis was shown in Figure.9.

In addition to the activation of cGAS-sting pathway, we explored whether CAF-secreted CXCL1 influenced the functions of other immune cells such as neutrophil and macrophage, which are abundant in the microenvironment. As shown in Figure.8G, neutrophil extracellular traps (NETs) which were highlighted as a promoter of tumor metastasis were observed in neutrophils which were co-cultured with CAFs where CXCL1 was overexpressed. Meanwhile, overexpression of CXCL in CAFs promoted the transition of pro-tumor M2 macrophages and recruited M2 macrophages(Figure.8H, 8I). These results suggested that esophageal cancer cells induced the up-regulation of CXCL1 in CAFs, which then established an immunosuppressive microenvironment via several mechanisms.

Discussion

The metastasis of tumor is a severely tough problem for the treatment of ESCC patients. There have been increasing studies which were focused on the mechanisms of ESCC metastasis [19-21]. However, the majority of these studies paid attention only to tumor cells during ESCC metastasis. Factually, the metastasis of tumors is not a spontaneous process but relies on the cooperation of several types of stromal cells

such as CAFs and immune cells [22-24]. As reported, the composition of tumor microenvironment (TME) in metastatic tumors is significantly different compared with that in primary tumors, suggesting that the TME was closely associated with tumor progression [25-27]. In metastatic tumors, the percentage of CAFs is higher than that in primary tumors [28-30]. Only tumor cells which were spatially closer to myofibroblastic CAFs (myCAFs), one major subtype of CAFs underwent epithelial to mesenchymal transition (EMT) to acquire the invasive phenotype [31, 32]. Furthermore, the subtypes of CAFs determine the organs of the tumor cells metastasize to, highlighting the determinative roles of CAFs in tumor metastasis [33]. Therefore, our study aimed to discover the role of CAFs in ESCC metastasis and explore novel strategy against ESCC metastasis.

In our study, CAFs were found to enhance the invasion ability of several ESCC cells. Upon co-culture with CAFs, the Hippo signaling pathway in ESCC cells is significantly changed with YAP translocated into the nucleus to initiate the transcription of downstream target genes such as SERPINE1 and AREG. In ESCC, YAP is highlighted as an attractive target because of its involvement in tumor migration, invasion, proliferation, cell stemness, apoptosis, therapeutic resistance, and immunity [34]. Our study found CAFs enhanced the malignant phenotype of ESCC cells through activating the YAP signaling, again emphasizing the importance of this pathway in ESCC treatment. In vivo, CAFs also induced the activation of YAP signaling and promoted lymphatic and pulmonary metastasis of ESCC cells. The immunohistochemical results confirmed that CAFs were located in the invasive edge of tumor tissues. This finding may support the the theory that CAFs drive tumor metastasis by generating a track through the matrix through which tumor cells invade behind fibroblasts. Inside tumor tissues, we found tumor cells were surrounded by a layer of CAFs. So, CAFs provided physical barrier for tumor cells to avoid the cell-killing effect of chemoradiotherapy as well as the immune surveillance. In the invasive ESCC tissues, we found there were a large number of neutrophils and M2 type macrophages both of which were evidenced to support ESCC metastasis [35, 36]. To discover the critical signaling pathway that controlled the tumor-promoting phenotype of CAFs, we performed scRNA-seq and high-throughput screening of 157 kinase inhibitors using CCK8 assay. We found IGFBP5 was highly expressed in a subpopulation of CAFs and facilitated IGF-2 secretion to promote ESCC metastasis. IGF-2 belongs to the IGF family and is involved in various aspects of cancer cells including the proliferation, migration and invasion, stemness maintenance and immune escape [37]. However, the role of IGF-2 in CAFs is less studied. Our study discovered that IGF-2 was predominantly expressed in CAFs and governed the crosstalk of CAFs and ESCC cells. In addition to our findings, Daqiang Song et al also confirmed that IGF-2 signaling was primarily sourced from CAFs in triple negative breast cancer (TNBC) and colon adenocarcinoma (COAD) [38]. They found that CAFs-secreted IGF-2 prevented the infiltration of cytotoxic $CD8^+$ T cells via CXCL12 and programmed death ligand 1 (PD-L1). By RNA-seq, we found IGF-2 in ESCC CAFs mainly regulated the expressions of Cyclin D1, a crucial cell cycle regulator. Furthermore, IGF-2 was responsible for CAFs activation and increased

glycolysis, promoting energy production which is essential for ESCC metastasis. On the other hand, lactate as a major metabolite of glycolysis, can enhance the infiltration and immunosuppressive activity of regulatory immune cells while suppressing the survival and cytotoxic function of antitumor immune cells, thereby contributing to tumor progression [39]. Therefore, we speculated that IGF-2-induced glycolysis activation may contribute to an establishment of immunosuppressive microenvironment through several mechanisms.

Since CAFs and tumor cells were reciprocally influenced, our study explored the effect of ESCC cells on CAFs during the metastasis. We found ESCC cells reshaped CAFs to establish an immunosuppressive microenvironment to enhance metastasis by up-regulating CXCL1. CXCL1 is recognized as important immune modulator by recruiting neutrophils [40]. Furthermore, CXCL1 was able to recruit M2 type macrophages and induce a phenotypic transition from anti-tumor M1 macrophages to pro-tumor M2 macrophages [41, 42]. Our study demonstrated that high secretion of CXCL1 in CAFs promoted the formation of neutrophil Extracellular Traps (NETs) by neutrophils and induced the transition of M2 macrophages. Hiromu Fujita et al previously reported peritumoral CD16b-positive neutrophil accumulation was an independent factor for lymph node metastasis for ESCC patients [43]. However, blood neutrophil counts did not correlate with lymph node metastasis. This difference may suggest that only those recruited neutrophils but not blood neutrophils affected tumor immune evasion. Our study may explain how ESCC tumor tissues recruited neutrophils to promote metastasis. Furthermore, NETs which are protein-decorated DNA webs were extensively studied due to their involvement in tumor metastasis. As reported, NETs can facilitate cancer invasion, migration, metastasis through several mechanisms including promoting premetastatic niche formation, interacting with circulating cancer cells, and inducing epithelial to mesenchymal transition [44]. So, CXCL1-promoted NETs may have important roles in ESCC metastasis.

We then found CAFs-secreted CXCL1 initiated the activation of cGAS-sting pathway, inducing the transcription of several immunosuppressive genes such as PD-L1, IL-8 and IL1β. As a immune regulatory pathway, the activation of cGAS-sting signaling can inhibit or promote cancer progression according to the cell types or pathological conditions [45]. When it is activated in CAFs, it may potentiate the tumor-promoting effect of CAFs. Consistent with our study, Jiale Liu et also found ovarian cancer cells initiated the activation of cGAS-sting in CAFs, promoting IFNB1 release, which caused platinum resistance [46]. Their study highlighted high expression of sting in CAFs as a poor prognostic factor. Our study found inhibition of cGAS-sting activation in CAFs could significantly decrease the expressions of PD-L1, IL-8 and IL1β, all of which contributed to the establishment of immunosuppressive microenvironment by attenuating the cytotoxicity of $CD8^+$ T cells and recruiting immunosuppressive cells such as MDSCs and TAMs [47, 48]. In addition to immune cells, CXCL1 and IL8 can directly induce angiogenesis by binding to CXCR2 on endothelial cells [49]. So, CAFs promoted the metastasis of ESCC tumors mainly through several mechanisms and during this process, several types of stromal cells acted together.

Together, our study discovered the complicate interaction of CAFs and ESCC cells during tumor metastasis and the involved mechanisms. We proposed the IGF-2 signaling as a critical target to reduce the malignant phenotype of ESCC cells promoted by CAFs. These finding may help better understand the nature of ESCC metastasis to develop novel anti-cancer strategy.

Conclusions

Together, our study discovered that the interaction of CAFs and esophageal cancer cells established a pro-metastatic microenvironment by paracrine IGF-2 signaling through several mechanisms. These findings in our study may aid in deeper understanding of the association of CAFs and tumor metastasis and shed novel lights into the development of anti-ESCC metastasis strategies.

Declarations

Ethics approval and consent to participate

This study has been approved by the ethical approval of Hangzhou Cancer Hospital. All of the patients participating in the study have signed informed consent.

Consent for publication

Not applicable.

Availability of data and materials

The data are available upon reasonable request from the corresponding author.

Competing interests

The authors declare no conflict of interests.

Funding

This work was financially supported by National Natural Science Foundation of China (No.82472935), Zhejiang Medicine and Health Science and Technology Project (No.WKJ-ZJ-2549, No.2024KY204, No.2023KY193 and No.2025KY1114) and The Construction Fund of Key Medical Disciplines of Hangzhou.

Authors' contributions

Jing Yue, Shuilian Wu, Zhifeng Tian and Rongjing Zhou performed most of the experiments and wrote the manuscript. Liqing Qiu, Jiajia Jin and Ruoqi Wang participated in animal studies. Tingting Zhang and Yiping Xu performed pathological examinations. Mingfeng Jiang and Bing Xia searched the literature. Hongfang Zhang revised and approved the manuscript.

References

[1] C. Yu, D. Zhang, C. Chen, S. Xing, P. Li, Y. Zhang, L. Shang, H. Ma, J. Zhou, Neoadjuvant immunotherapy for resectable esophageal cancer: Research progress and clinical perspectives, Critical reviews in oncology/hematology, 221 (2026) 105191.

[2] X. Tong, M. Jin, L. Wang, D. Zhang, Y. Yin, Q. Shen, Prognostic biomarkers for immunotherapy in esophageal cancer, Frontiers in immunology, 15 (2024) 1420399.

[3] J.K. Waters, S.I. Reznik, Update on Management of Squamous Cell Esophageal Cancer, Current oncology reports, 24 (2022) 375-385.

[4] H.C. Puhr, G.W. Prager, A. Ilhan-Mutlu, How we treat esophageal squamous cell carcinoma, ESMO open, 8 (2023) 100789.

[5] W. Dai, J.M. Ko, V.Z. Yu, Z. Hou, L.K. Chow, M.K.Y. Chung, K.A. Islam, B.H. Ng, C.W. Wong, K.K. Leung, C. Chen, I.Y.H. Wong, S.Y. Law, A.W. Lo, A.K. Lam, M.L. Lung, Characterizing chromosome instability reveals its association with lipid-associated macrophages and clonal evolution of lymph node metastasis in esophageal squamous cell carcinoma, Cancer letters, 628 (2025) 217874.

[6] H. Yang, H. Liu, Y. Chen, C. Zhu, W. Fang, Z. Yu, W. Mao, J. Xiang, Y. Han, Z. Chen, H. Yang, J. Wang, Q. Pang, X. Zheng, H. Yang, T. Li, F. Lordick, X.B. D'Journo, R.J. Cerfolio, R.J. Korst, N.M. Novoa, S.J. Swanson, A. Brunelli, M. Ismail, H.C. Fernando, X. Zhang, Q. Li, G. Wang, B. Chen, T. Mao, M. Kong, X. Guo, T. Lin, M. Liu, J. Fu, Neoadjuvant Chemoradiotherapy Followed by Surgery Versus Surgery Alone for Locally Advanced Squamous Cell Carcinoma of the Esophagus (NEOCRTEC5010): A Phase III Multicenter, Randomized, Open-Label Clinical Trial, Journal of clinical oncology : official journal of the American Society of Clinical Oncology, 36 (2018) 2796-2803.

[7] B.M. Eyck, J.J.B. van Lanschot, M. Hulshof, B.J. van der Wilk, J. Shapiro, P. van Hagen, M.I. van Berge Henegouwen, B.P.L. Wijnhoven, H.W.M. van Laarhoven, G.A.P. Nieuwenhuijzen, G.A.P. Hospers, J.J. Bonenkamp, M.A. Cuesta, R.J.B. Blaisse, O.R. Busch, G.M. Creemers, C.J.A. Punt, J.T.M. Plukker, H.M.W. Verheul, E.J. Spillenaar Bilgen, M.J.C. van der Sangen, T. Rozema, F.J.W. Ten Kate, J.C. Beukema, A.H.M. Piet, C.M. van Rij, J.G. Reinders, H.W. Tilanus, E.W. Steyerberg, A. van der Gaast, Ten-Year Outcome of Neoadjuvant Chemoradiotherapy Plus Surgery for Esophageal Cancer: The Randomized Controlled CROSS Trial, Journal of clinical oncology : official journal of the American Society of Clinical Oncology, 39 (2021) 1995-2004.

[8] Y. Li, Y. Zheng, J. Huang, R.C. Nie, Q.N. Wu, Z. Zuo, S. Yuan, K. Yu, C.C. Liang, Y.Q. Pan, B.W. Zhao, Y. Xu, Q. Zhang, Y. Zheng, J. Chen, Z.L. Zeng, W. Wei, Z.X. Liu, R.H. Xu, H.Y. Luo, CAF-macrophage crosstalk in tumour microenvironments governs the response to immune checkpoint blockade in gastric cancer peritoneal metastases, Gut, 74 (2025) 350-363.

[9] P. Isaacsson Velho, D.A. Bastos, P.T. Saint'ana, B. Rigatti, E.T. da Costa, D.Q.B. Muniz, F. Andreis, R.D.P. Ferreira, L. Giongo Pedrotti, S. Maistro, M.L.H. Katayama, M. Folgueira, A. Morelle, A. Leal, G. de Castro, Jr., Nivolumab in Patients with Metastatic Castration-Resistant Prostate Cancer with and without DNA Repair

Defects, Clinical cancer research : an official journal of the American Association for Cancer Research, 30 (2024) 5342-5352.
[10] Z. Liu, J. Chen, Y. Ren, S. Liu, Y. Ba, A. Zuo, P. Luo, Q. Cheng, H. Xu, X. Han, Multi-stage mechanisms of tumor metastasis and therapeutic strategies, Signal transduction and targeted therapy, 9 (2024) 270.
[11] M. El-Tanani, S.A. Rabbani, R. Babiker, I. Rangraze, S. Kapre, S.S. Palakurthi, A.M. Alnuqaydan, A.A. Aljabali, M. Rizzo, Y. El-Tanani, M.M. Tambuwala, Unraveling the tumor microenvironment: Insights into cancer metastasis and therapeutic strategies, Cancer letters, 591 (2024) 216894.
[12] G. Caligiuri, D.A. Tuveson, Activated fibroblasts in cancer: Perspectives and challenges, Cancer cell, 41 (2023) 434-449.
[13] J.D. Domogauer, S.M. de Toledo, R.W. Howell, E.I. Azzam, Acquired radioresistance in cancer associated fibroblasts is concomitant with enhanced antioxidant potential and DNA repair capacity, Cell communication and signaling : CCS, 19 (2021) 30.
[14] C. Gaggioli, S. Hooper, C. Hidalgo-Carcedo, R. Grosse, J.F. Marshall, K. Harrington, E. Sahai, Fibroblast-led collective invasion of carcinoma cells with differing roles for RhoGTPases in leading and following cells, Nature cell biology, 9 (2007) 1392-1400.
[15] L. Patras, L. Shaashua, I. Matei, D. Lyden, Immune determinants of the pre-metastatic niche, Cancer cell, 41 (2023) 546-572.
[16] L. Arpinati, R. Scherz-Shouval, From gatekeepers to providers: regulation of immune functions by cancer-associated fibroblasts, Trends in cancer, 9 (2023) 421-443.
[17] L. Qiu, J. Yue, L. Ding, Z. Yin, K. Zhang, H. Zhang, Cancer-associated fibroblasts: An emerging target against esophageal squamous cell carcinoma, Cancer letters, 546 (2022) 215860.
[18] Y. Meng, L. Yang, X. Wei, H. Luo, Y. Hu, X. Tao, J. He, X. Zheng, Q. Xu, K. Luo, G. Yu, Q. Luo, CCT5 interacts with cyclin D1 promoting lung adenocarcinoma cell migration and invasion, Biochemical and biophysical research communications, 567 (2021) 222-229.
[19] Z. Jiang, Y. Yang, J. Zhou, X. Li, Q. Meng, X. Yu, Y. Xue, M. Li, Y. Cai, P. Han, M. Jiang, H. Wang, C. Liu, J. Zhao, L. Wan, D. Bao, Targeting Drp1 inhibits ESCC progression via the ROS-PGC1-α-Nrf1/2 pathway, Journal of translational medicine, 23 (2025) 674.
[20] J. Chen, J. Zhang, Y. Zhu, Y. Zhu, J. Pang, Q. Wu, Y. Wang, Q. Zhan, Focal adhesion kinase/Src family kinase axis-mediated tyrosine phosphorylation of metabolic enzymes facilitates tumor metastasis, Signal transduction and targeted therapy, 10 (2025) 280.
[21] J. Chen, J. Chen, X. Lv, X. Chen, L. Ming, X. Huang, F. Wen, H. Tang, Q. Gao, C. Liu, J. Weng, Z. Huang, Y. Zheng, F. Lin, W. Chen, X. Shang, C. Yu, Y. Huang, Cancer-derived fucosylated exosomal miR-6842-3p as a novel marker promotes ESCC angiogenesis and metastasis via the PTEN/AKT/mTOR/IRF1/CXCL10 axis, Oncogene, 45 (2026) 104-120.

[22] X. Mao, J. Xu, W. Wang, C. Liang, J. Hua, J. Liu, B. Zhang, Q. Meng, X. Yu, S. Shi, Crosstalk between cancer-associated fibroblasts and immune cells in the tumor microenvironment: new findings and future perspectives, Molecular cancer, 20 (2021) 131.
[23] B. Xia, L. Qiu, J. Yue, J. Si, H. Zhang, The metabolic crosstalk of cancer-associated fibroblasts and tumor cells: Recent advances and future perspectives, Biochimica et biophysica acta. Reviews on cancer, 1879 (2024) 189190.
[24] L. Ding, Z. Li, J. Yue, L. Qiu, Z. Tian, H. Zhang, Cancer-associated fibroblasts as a critical driver in tumor metastasis: The mechanisms and future perspectives, iScience, 29 (2026) 114788.
[25] S. Liu, Z. Zhang, Z. Wang, C. Liu, G. Liang, T. Xu, Z. Li, X. Duan, G. Xu, X. Feng, Q. Feng, Q. Wang, D. Han, C. Zhang, J. Li, L. Shen, SPP1 Drives Colorectal Cancer Liver Metastasis and Immunotherapy Resistance by Stimulating CXCL12 Production in Cancer-Associated Fibroblasts, Cancer research, 86 (2026) 58-79.
[26] A.M. Khaliq, M. Rajamohan, O. Saeed, K. Mansouri, A. Adil, C. Zhang, A. Turk, J.L. Carstens, M. House, S. Hayat, G.P. Nagaraju, S.G. Pappas, Y.A. Wang, N.J. Zyromski, M. Opyrchal, K.P. Lee, H. O'Hagan, B. El Rayes, A. Masood, Spatial transcriptomic analysis of primary and metastatic pancreatic cancers highlights tumor microenvironmental heterogeneity, Nature genetics, 56 (2024) 2455-2465.
[27] F. Ozmen, T.Y. Ozmen, A. Ors, M. Janghorban, M.J. Rames, X. Li, A.R. Doe, F. Behbod, G.B. Mills, H. Mohammed, Single-cell RNA sequencing reveals different cellular states in malignant cells and the tumor microenvironment in primary and metastatic ER-positive breast cancer, NPJ breast cancer, 11 (2025) 95.
[28] H. Shi, H. Tian, T. Zhu, Q. Liao, C. Liu, P. Yuan, Y. Li, J. Yang, C. Zong, S. Jia, J. Ruan, S. Ge, R. Jia, P. Chai, S. Xu, X. Fan, Single-cell sequencing depicts tumor architecture and empowers clinical decision in metastatic conjunctival melanoma, Cell discovery, 10 (2024) 63.
[29] T.Y. Lai, T.C. Chiang, C.Y. Lee, T.C. Kuo, C.H. Wu, Y.I. Chen, C.M. Hu, M. Maskey, S.C. Tang, Y.M. Jeng, Y.W. Tien, E.Y.P. Lee, W.H. Lee, Unraveling the impact of cancer-associated fibroblasts on hypovascular pancreatic neuroendocrine tumors, British journal of cancer, 130 (2024) 1096-1108.
[30] Y. Wang, X. Li, Q. Gang, Y. Huang, M. Liu, H. Zhang, S. Shen, Y. Qi, J. Zhang, Pathomics and single-cell analysis of papillary thyroid carcinoma reveal the pro-metastatic influence of cancer-associated fibroblasts, BMC cancer, 24 (2024) 710.
[31] H. Allgayer, S. Mahapatra, B. Mishra, B. Swain, S. Saha, S. Khanra, K. Kumari, V.K. Panda, D. Malhotra, N.S. Patil, J.H. Leupold, G.C. Kundu, Epithelial-to-mesenchymal transition (EMT) and cancer metastasis: the status quo of methods and experimental models 2025, Molecular cancer, 24 (2025) 167.
[32] Z. Ye, Q. Li, Y. Hu, H. Hu, J. Xu, M. Guo, W. Zhang, X. Lou, Y. Wang, H. Gao, D. Jing, G. Fan, Y. Qin, Y. Zhang, X. Chen, J. Chen, X. Xu, X. Yu, M. Liu, S. Ji, The stromal microenvironment endows pancreatic neuroendocrine tumors with spatially specific invasive and metastatic phenotypes, Cancer letters, 588 (2024) 216769.
[33] K. Xu, H. Wang, Y.X. Zou, H.H. Zhang, Y.N. Wang, X.R. Ren, H.Q. Wang, Y.H. Xu, J.J. Li, H. Tang, C. He, S. Wei, T. Tian, L.L. Li, H. Zhou, L.J. Xu, J.W. Fang, C.

Guo, J.X. Yang, Y.Y. Zhou, Z.H. Zhang, Y.Y. Pan, Distinct fibroblast subpopulations associated with bone, brain or intrapulmonary metastasis in advanced non-small-cell lung cancer, Clinical and translational medicine, 14 (2024) e1605.
[34] W. Wang, T. Chang, L. Wang, R. Bin Mohamed, N.H. Binti Ahmad, X. Li, YAP as a therapeutic target in esophageal squamous cell carcinoma: insights and strategies, Annals of medicine, 57 (2025) 2536200.
[35] J. Tang, B. Qi, Q. Zhuo, S. Huo, X. Dang, T. Pang, K. Cao, Y. Liu, B. Zhao, Acetyl-CoA carboxylase 1 knockdown promotes esophageal squamous cell carcinoma metastasis via the CXCL8-NET axis, Communications biology, 8 (2025) 1609.
[36] Y. Sun, Y. Qian, C. Chen, H. Wang, X. Zhou, W. Zhai, L. Qiu, X. Zhou, H. Ning, Y. Zhao, C. Shi, L. Han, Y. Qi, Y. Wu, Y. Gao, Extracellular vesicle IL-32 promotes the M2 macrophage polarization and metastasis of esophageal squamous cell carcinoma via FAK/STAT3 pathway, Journal of experimental & clinical cancer research : CR, 41 (2022) 145.
[37] A. Belfiore, R.V. Rapicavoli, R. Le Moli, R. Lappano, A. Morrione, E.M. De Francesco, V. Vella, IGF2: A Role in Metastasis and Tumor Evasion from Immune Surveillance?, Biomedicines, 11 (2023).
[38] D. Song, Y. Wu, J. Li, J. Liu, Z. Yi, X. Wang, J. Sun, L. Li, Q. Wu, Y. Chen, H. Fang, T. Luan, H. Du, J. Huang, W. Peng, Y. Wei, F. Li, Q. Li, L. Zhang, Y. Zhu, J. Wan, G. Ren, H. Li, Insulin-like growth factor 2 drives fibroblast-mediated tumor immunoevasion and confers resistance to immunotherapy, The Journal of clinical investigation, 134 (2024).
[39] J. Chen, Z. Huang, Y. Chen, H. Tian, P. Chai, Y. Shen, Y. Yao, S. Xu, S. Ge, R. Jia, Lactate and lactylation in cancer, Signal transduction and targeted therapy, 10 (2025) 38.
[40] Q. Wang, X. Zhang, C. Han, Z. Lv, Y. Zheng, X. Liu, Z. Du, T. Liu, D. Xue, T. Li, L. Wang, Immunodynamic axis of fibroblast-driven neutrophil infiltration in acute pancreatitis: NF-κB-HIF-1α-CXCL1, Cellular & molecular biology letters, 30 (2025) 57.
[41] Z. Xu, J. Si, A. Liang, Y. Zhang, J. Gong, G. Li, Y. Zhong, M. Yu, R. Feng, X. Li, J. Chang, N. Wang, The chemosensitizing activity of betulinic acid in suppressing macrophage polarization through GSK-3β/β-catenin/CXCL1 signaling in breast cancer, Phytomedicine : international journal of phytotherapy and phytopharmacology, 148 (2025) 157304.
[42] S. Leypold, J. Riese, L. Seillier, M. Kühnel, J. Pannhausen, C.O.J. Fröhlich, C. Martin, P. Boor, M. Saar, D.D. Jonigk, N.T. Gaisa, M. Rose, Tumor-stromal crosstalk and macrophage enrichment are associated with chemotherapy response in bladder cancer, FEBS open bio, (2025).
[43] H. Fujita, S. Motoyama, J. An, Y. Nagakai, T. Yamaguchi, S. Koyota, Y. Sato, A. Wakita, K. Imai, K. Kuba, Y. Minamiya, Peritumoral CD16b positive-neutrophil accumulation strongly correlates with regional lymph node metastasis in thoracic esophageal squamous cell cancer, Surgery, 171 (2022) 1535-1542.
[44] J.M. Adrover, X. Han, L. Sun, T. Fujii, N. Sivetz, J. Daßler-Plenker, C. Evans, J. Peters, X.Y. He, C.D. Cannon, W.J. Ho, G. Raptis, R.S. Powers, M. Egeblad,

Neutrophils drive vascular occlusion, tumour necrosis and metastasis, Nature, 645 (2025) 484-495.
[45] A. Shim, Y. Chen, J. Maciejowski, Activation and regulation of cGAS-STING signaling in cancer cells, Molecular cell, 85 (2025) 3807-3822.
[46] J. Liu, C. Liu, Y. Ma, X. Pan, R. Chu, S. Yao, J. Chen, C. Liu, Z. Chen, C. Sheng, K. Zhang, Y. Xue, H.B. Schiöth, B. Kong, Q. Zhang, K. Song, STING inhibitors sensitize platinum chemotherapy in ovarian cancer by inhibiting the CGAS-STING pathway in cancer-associated fibroblasts (CAFs), Cancer letters, 588 (2024) 216700.
[47] J.W. Chen, J.Y. Li, H.Q. Feng, L.M. Fu, X.W. Zhou, H.S. Lin, Y.H. Wang, K.Z. Liu, Y.H. Chen, Z. Wang, Q. Deng, J.Y. Wang, M.Y. Jin, H. Liang, J.H. Wei, J.H. Luo, C.P. Gui, FKBP10 promotes M2 polarization of macrophage via MEK/ERK/CXCL8 axis and facilitates tumor progression in clear cell renal cell carcinoma, International journal of biological sciences, 22 (2026) 1807-1833.
[48] H. Liu, Q. Zhao, L. Tan, X. Wu, R. Huang, Y. Zuo, L. Chen, J. Yang, Z.X. Zhang, W. Ruan, J. Wu, F. He, Y. Fang, F. Mao, P. Zhang, X. Zhang, P. Yin, Z. Yan, W. Xu, H. Lu, Q. Li, M. Liang, Y. Jia, C. Chen, S. Xu, Y. Shi, Y.F. Ping, G.J. Duan, X.H. Yao, Z. Han, T. Pang, Y. Cui, X. Zhang, B. Zhu, C. Qi, Y. Wang, S.Q. Lv, X.W. Bian, X. Liu, Neutralizing IL-8 potentiates immune checkpoint blockade efficacy for glioma, Cancer cell, 41 (2023) 693-710.e698.
[49] M.J. Garcia, A.L. Beall, M.S. Morales, N.J. Beatty, S.A. Palmer, M. Jhala, A. Drmanovic, S. Priest, Y. Zhang, R. Yang, K. Arellano, J.S. Penn, D.A. Padovani-Claudio, IL-8 receptor signaling as a novel target for angiogenic retinopathies, Angiogenesis, 29 (2025) 2.

Figure legends

Figure.1 CAFs promoted the invasion of ESCC cells by inducing epithelial to mesenchymal (EMT) transition through activating YAP signaling. A. The invasion ability of esophageal cancer cells which were co-cultured with or without (control) CAFs as detected by transwell assay. The quantitative analysis of invaded cells under indicated culture conditions was shown in the right panel. **P<0.01, ****P<0.0001. B. Volcano map of the gene signature of ESCC cells co-cultured with CAFs and GSEA (Gene set enrichment analysis) revealed significant enrichment of EMT transition. C. The heatmap of genes involved in EMT phenotype including epithelial markers, mesenchymal markers, ECM degrading enzymes and transcription factors in ESCC cells which were co-cultured with or without CAFs. D. KEGG analysis of the differentially expressed genes in ESCC cells which were co-cultured with CAFs as detected by RNA-seq. The red box indicated that Hippo signaling pathway was significantly changed in ESCC cells. E. Immunofluorescence analysis of YAP expression in ESCC cells which were co-cultured with or without CAFs (control). F. qRT-PCR analysis of AREG and SERPINE1 expressions, both of which are downstream genes of YAP signaling, in ESCC cells which were co-cultured with or without CAFs (control). ****P<0.0001. G. qRT-PCR analysis of YAP expression in CAFs which were transfected with YAP siRNA (siYAP) or scrambled siRNA (Negative control, NC). ****P<0.0001. H. The invasion ability of ESCC cells which were transfected with scrambled siRNA (Negative Control, NC) or YAP siRNA (siYAP) before co-culture with CAFs. *P<0.05, **P<0.01, ***P<0.001.

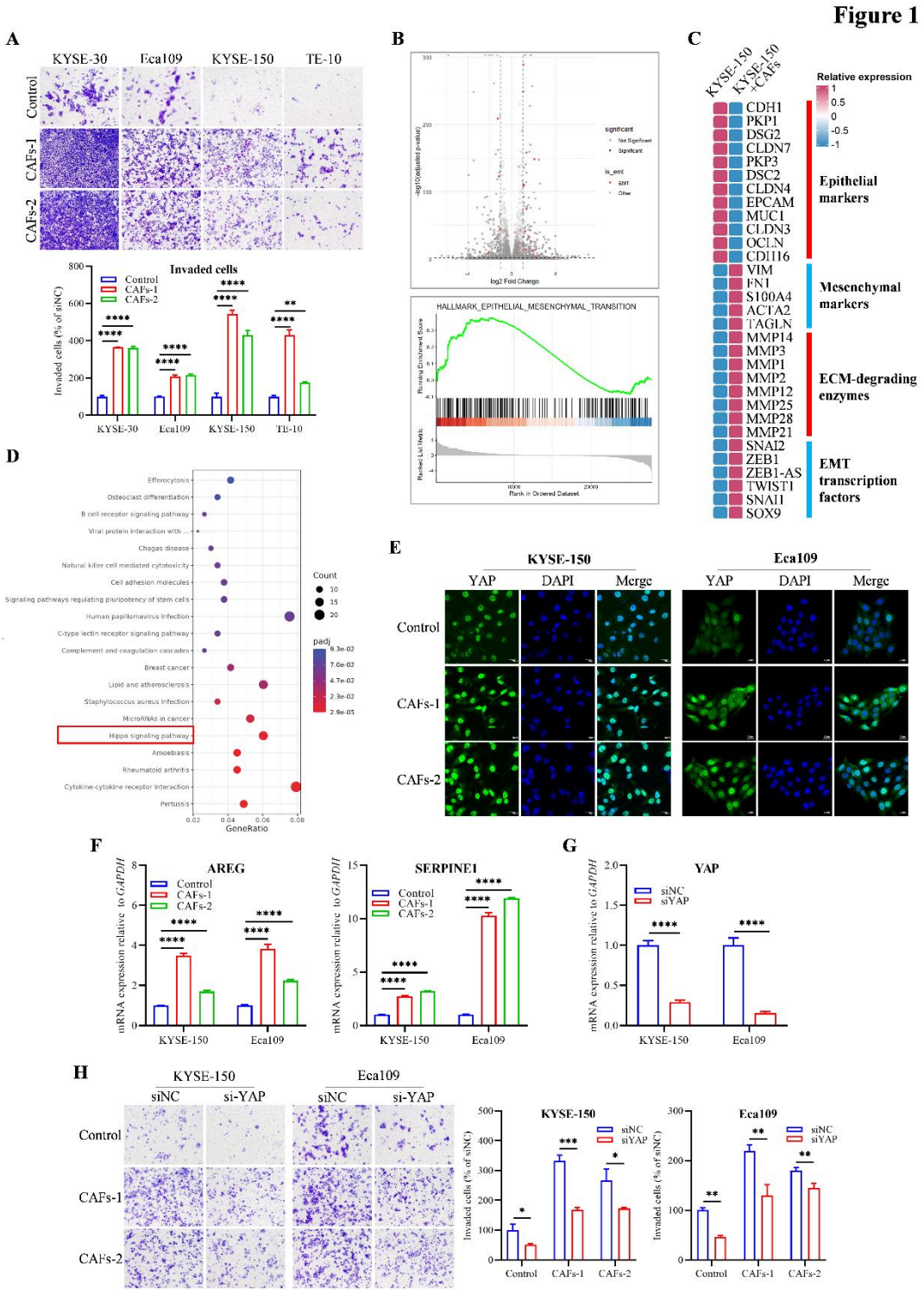


Figure. 2 CAFs promoted lymphatic and pulmonary metastasis of ESCC cell lines in vivo. A. and B. The photos of tumors (in situ) and lymph nodes (LNs) in the mice which were injected with tumor cells (A: KYSE-150; B: KYSE-30) alone or in combination of CAFs into foot pad. The right panel shows quantitative analysis of tumor weight and LNs size in the mice. **P<0.01, ***P<0.001, ****P<0.0001. C. and D. The HE and IHC staining of xenograft tumors in “A” and “B”. pan-CK: a marker of epithelial-derived tumors. The right panel shows the cases and metastatic

areas of metastatic tumors in the mice in “A” and “B”. *P<0.05, ***P<0.001. E. and F. The HE staining of the lungs in the mice into which tumor cells (E: KYSE-150; F: TE-10) alone or in combination of CAFs were injected by tail vein. The number of pulmonary nodules in the mice were also shown. *P<0.05. G. The IHC staining of α-SMA, a marker of CAFs activation, in the tumors (in situ) and lymph nodes (LNs) of mice which were injected with tumor cells alone or in combination of CAFs into foot pad. H. The IHC staining of Ly-6G, a marker of neutrophils and CD206, a marker of protumor M2 macrophages in the tumors (in situ) of mice which were injected with tumor cells alone or in combination of CAFs into foot pad. The positive area of Ly-6G and CD206 in the tumors was calculated using image J. *P<0.05, **P<0.01.

Figure 2

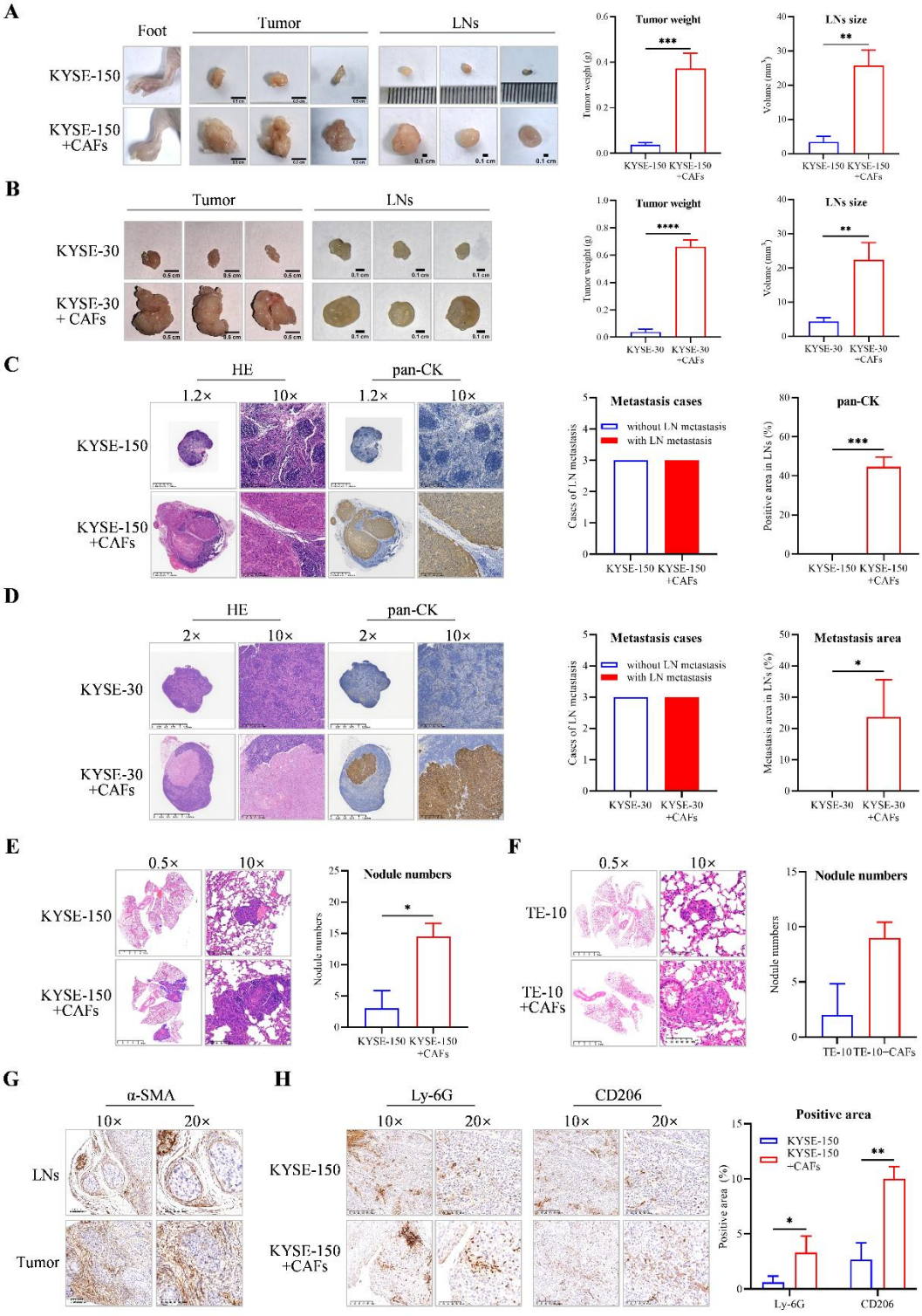


Figure. 3 High expression of IGFBP5 facilitated IGF-2 secretion in CAFs. A. The UMAP plot of clustered scRNA-seq data from ESCC CAFs. B. The GO analysis of CAFs subtype with high expression of IGFBP5. C. qRT-PCR analysis of IGFBP5 expression in CAFs, ESCC cells and normal esophageal epithelium cells Het-1A. D. qRT-PCR analysis of IGFBP5 expression in CAFs which were transfected with IGFBP5 siRNA (siIGFBP5) or scrambled siRNA (negative control, siNC). E. The

invasive ability of CAFs which were transfected with IGFBP5 siRNA (siIGFBP5) or scrambled siRNA (negative control, siNC) using transwell assay. F. qRT-PCR analysis of IGF-1 and IGF-2 expressions in CAFs, ESCC cells and normal esophageal epithelium cells Het-1A. G. qRT-PCR analysis of IGF-2 expression in CAFs which were transfected with IGFBP5 siRNA (siIGFBP5) or scrambled siRNA (negative control, siNC). H. Western blotting analysis of IGF-2 and IGFBP5 expressions in CAFs which were transfected with IGFBP5 siRNA (siIGFBP5) or scrambled siRNA (negative control, siNC).

Figure 3

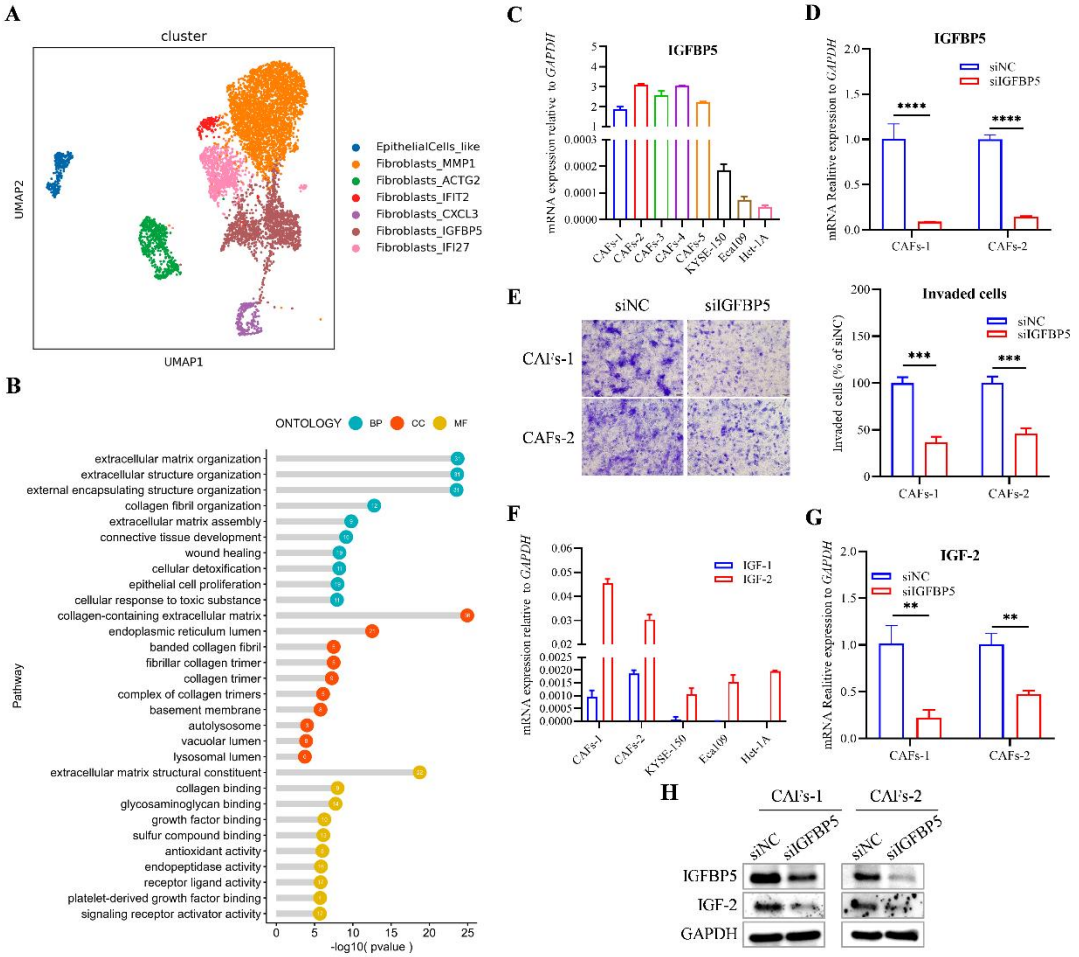


Figure. 4 The IGF-2 signaling secreted by CAFs promoted the invasion of ESCC cells by activating YAP. A. qRT-PCR analysis of IGF-1 and IGF-2 expressions in CAFs which were co-cultured with or without (control) ESCC cells for 48 h. *P<0.05, ***P<0.001, ****P<0.0001. B. Western blotting analysis of IGF-2 expression in CAFs which were co-cultured with or without (control) ESCC cells. GAPDH was used as a loading control. C. qRT-PCR analysis of IGF-2 expression in KYSE-150 and Eca109 which were co-cultured with or without (control) CAFs. **P<0.01, ****P<0.0001. D. qRT-PCR analysis of IGF-2 expression in CAFs which were transfected with IGF-2 siRNA (siIGF-2) or scrambled siRNA (negative control, siNC). ****P<0.0001. E. The invasive ability of CAFs which were transfected with IGF-2 siRNA (siIGF-2) or scrambled siRNA (negative control, siNC) using transwell assay.

**P<0.01. F. qRT-PCR analysis of YAP expression in ESCC cells co-cultured with CAFs which were transfected with IGF-2 siRNA (siIGF-2) or scrambled siRNA (negative control, siNC). G. The invasive ability of ESCC cells which were co-cultured with CAFs in which IGF-2 siRNA (siIGF-2) or scrambled siRNA (negative control, siNC) were transfected using transwell assay. *P<0.05, **P<0.01, ***P<0.001. H. Western blotting analysis of IGF-2, α-SMA and TGFβ-1 expressions in CAFs which were transfected with IGF-2 siRNA (siIGF-2) or scrambled siRNA (negative control, siNC). GAPDH was used as a loading control. I. The schematic diagram of high-throughput screening of 157 kinase inhibitors in CAFs. J. The cell viability of CAFs, ESCC cells and normal esophageal epithelium cells Het-1A exposed to GSK1838705A, an inhibitor of IGF-1R pathway using CCK8 assay.

Figure 4

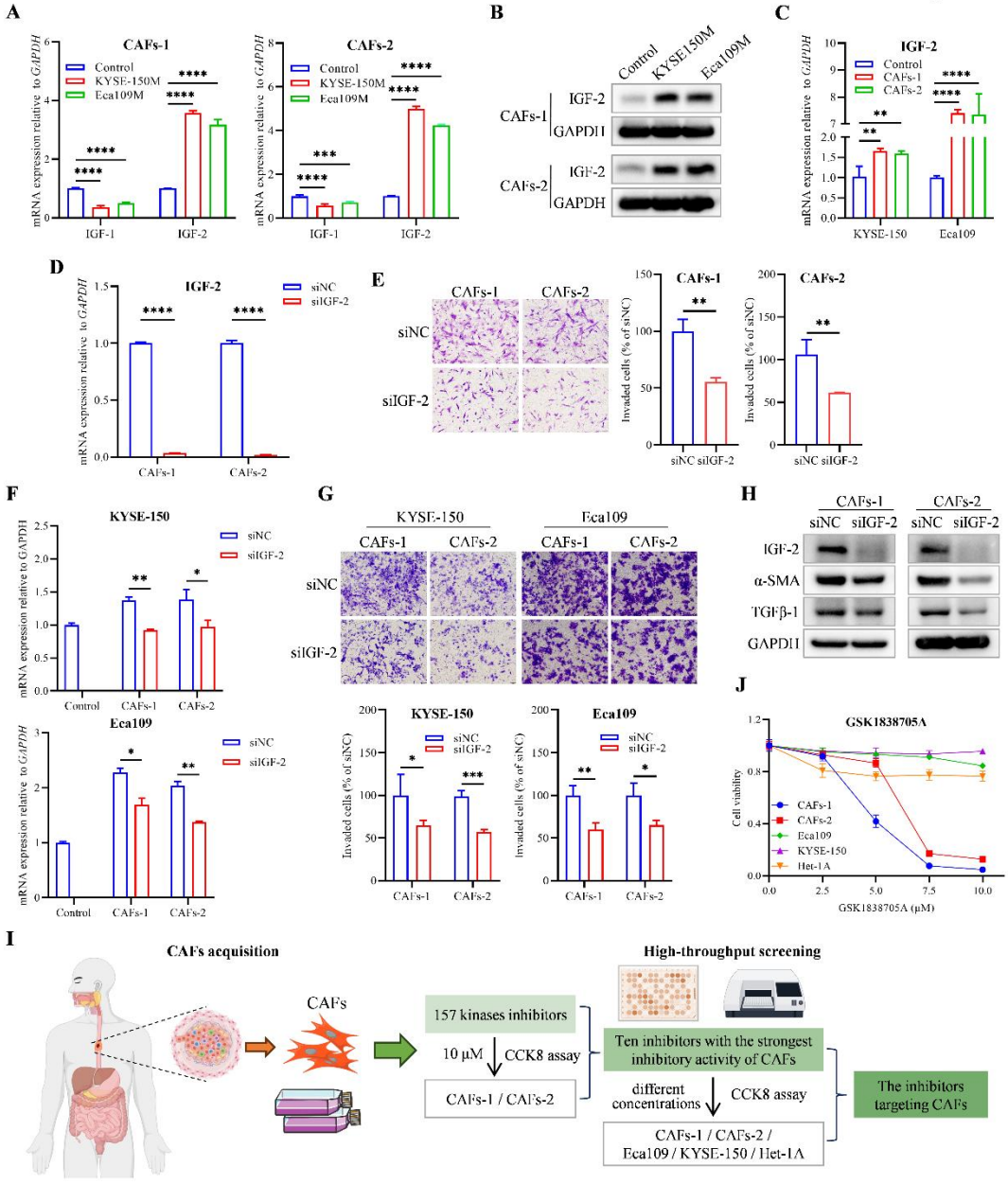


Figure.5 Inhibition of CAFs-secreted IGF-2 signaling attenuated tumor

metastasis in vivo. A. The photos of tumors in the foot pad of mice which were transfected with IGF-2 shRNA (IGF-2^{low}) or scrambled shRNA (control). The weight of tumors in the foot pad and the volume of lymph nodes (LNs) were also shown in the mice which were transfected with IGF-2 shRNA (IGF-2^{low}) or scrambled shRNA (control). **P<0.01, ***P<0.001. B. The HE and IHC staining of LNs in the mice which were transfected with IGF-2 shRNA (IGF-2^{low}) or scrambled shRNA (control). The metastasis area and pan-CK positive area in LNs were also shown in the mice which were transfected with IGF-2 shRNA (IGF-2^{low}) or scrambled shRNA (control). ***P<0.001. C. The HE and Ki-67 staining of pulmonary nodules in the mice which were transfected with IGF-2 shRNA (IGF-2^{low}) or scrambled shRNA (control) via tail vein. The largest diameter and Ki-67 positive area of pulmonary nodules were also shown. *P<0.05, **P<0.01. D. The IHC analysis of IGF-2, Ly-6G, a marker of neutrophils and CD206, a marker of protumor M2 macrophages in the tumors (in situ) of mice which were injected with IGF-2 shRNA (IGF-2^{low}) or scrambled shRNA (control) into foot pad. The positive area of IGF-2, Ly-6G and CD206 in the tumors was calculated using image G. *P<0.05, **P<0.01.

Figure 5

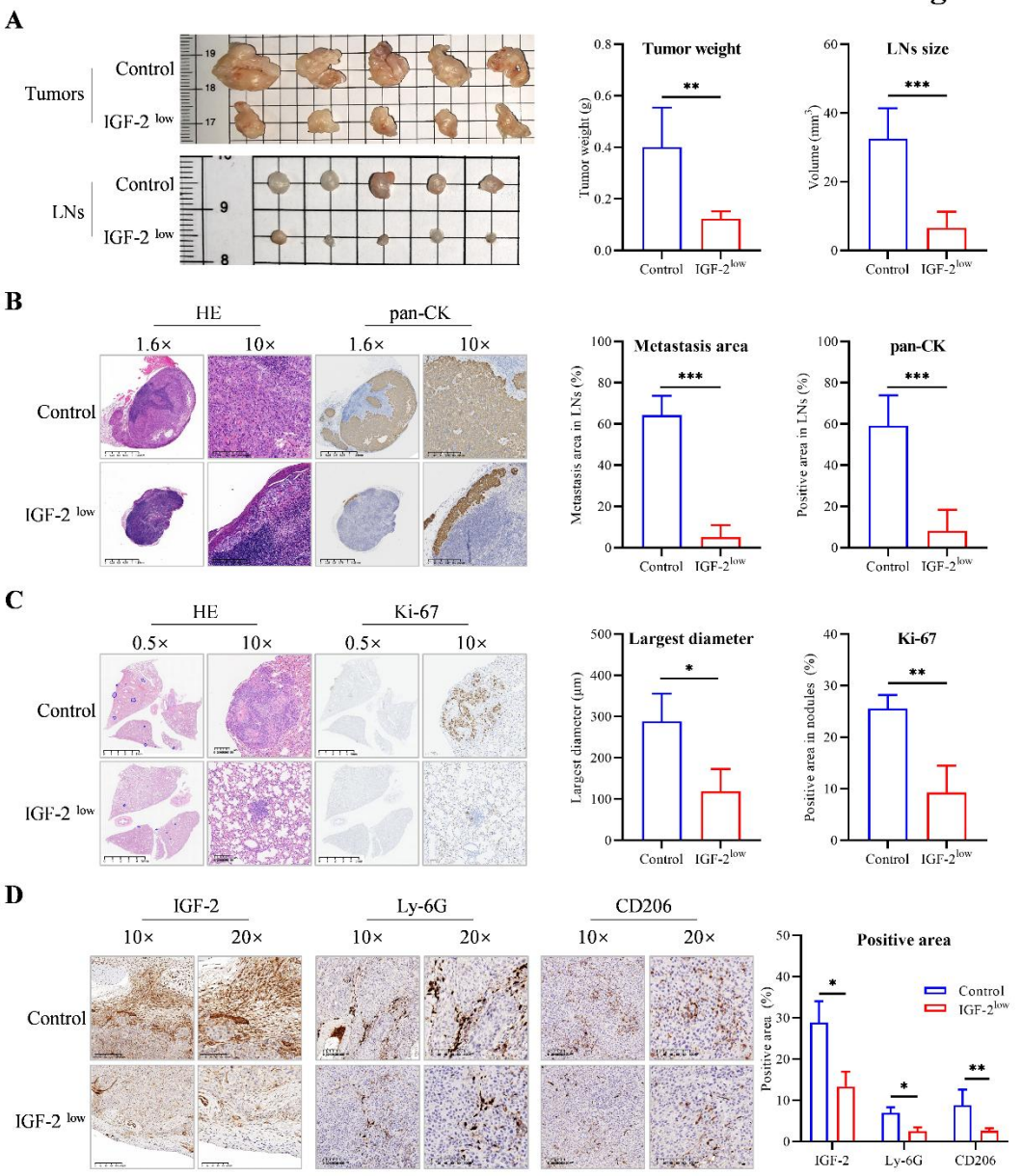


Figure.6 The IGF-2 signaling in CAFs regulated Cyclin D1 expression and glycolysis. A. KEGG analysis of the differentially expressed genes in CAFs which were transfected with IGF-2 siRNA. B. The heatmap of differentially expressed genes associated with cell cycle in CAFs which were transfected with IGF-2 siRNA. C. qRT-PCR analysis of Cyclin D1 expression in CAFs which were transfected with IGF-2 siRNA (siIGF-2) or scrambled siRNA (Negative control, siNC). ****P<0.0001. D. qRT-PCR analysis of Cyclin D1 expression in CAFs which were transfected with Cyclin D1 siRNA (siCyclin D1) or scrambled siRNA (Negative control, siNC). ****P<0.0001. E. Flow cytometry analysis of cell cycle distribution of CAFs which were transfected with Cyclin D1 siRNA (siCyclin D1) or scrambled siRNA (Negative control, siNC). *P<0.05, **P<0.01, ***P<0.001, ****P<0.0001. F. The cell proliferation of CAFs which were transfected with Cyclin D1 siRNA (siCyclin D1) or scrambled siRNA (Negative control, siNC) by CCK8 assay. ****P<0.0001. G.The

invasive ability of CAFs which were transfected with transfected with Cyclin D1 siRNA (siCyclin D1) or scrambled siRNA (Negative control, siNC). *P<0.05, ***P<0.001. H. The heatmap of differentially expressed genes associated with cell metabolism including glycolysis in CAFs which were transfected with IGF-2 siRNA (siIGF-2) or scrambled siRNA (Negative control, siNC). I. qRT-PCR analysis of the genes involved in the glycolysis in CAFs which were transfected with IGF-2 siRNA (siIGF-2) or scrambled siRNA (Negative control, siNC). *P<0.05, ****P<0.0001. J. The glucose or lactate concentration in the medium of CAFs which were transfected with IGF-2 siRNA (siIGF-2) or scrambled siRNA (Negative control, siNC). *P<0.05, **P<0.01, ****P<0.0001. K. qRT-PCR analysis of MCT4 and Cyclin D1 expressions in CAFs which were transfected with MCT4 siRNA (siMCT4) or scrambled siRNA (Negative control, siNC). ****P<0.0001.

Figure 6

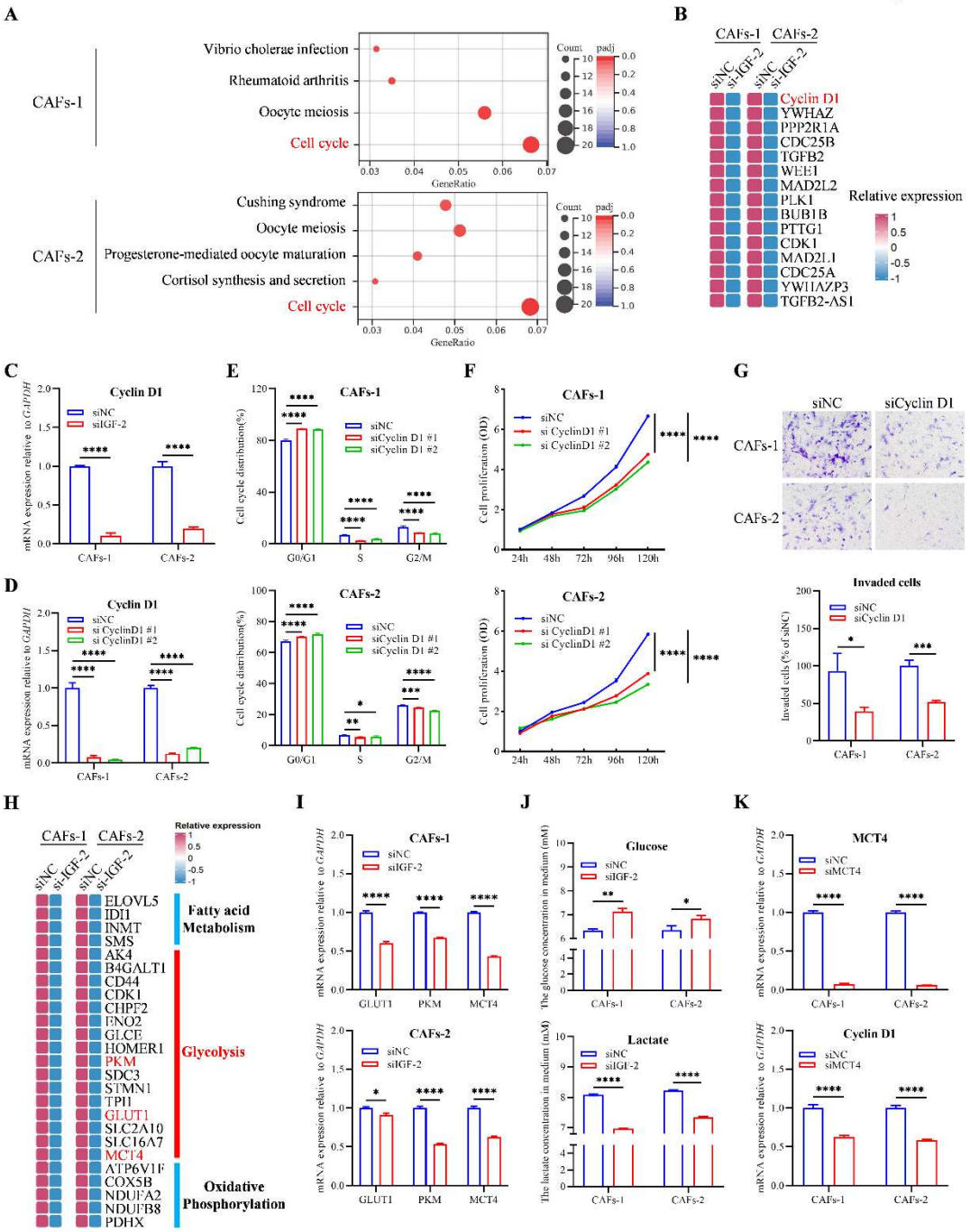


Figure.7 ESCC cells induced the inflammatory phenotype of CAFs. A. The KEGG analysis of the gene signature in CAFs which were co-cultured with ESCC cells. B. The volcano plot of differentially expressed genes in CAFs which were co-cultured with ESCC cells. Some of the significantly up-regulated chemokines were indicated. C. qRT-PCR analysis of IL1β and IL-8 expression in CAFs which were co-cultured with ESCC cells or not (control). KYSE-150M: KYSE-150 medium. Eca109M: Eca109 medium. ****P<0.0001. D. and E. The mRNA and protein expression of CXCL1 in CAFs which were co-cultured with ESCC cells or not (control) as detected by qRT-PCR and western blotting analysis, respectively.

GAPDH was used as a loading control. ****P<0.0001. F. qRT-PCR analysis of PD-L1 expression in CAFs and in ESCC cells which were co-cultured or not (control). KYSE-150M: KYSE-150 medium. Eca109M: Eca109 medium. ****P<0.0001.

Figure 7

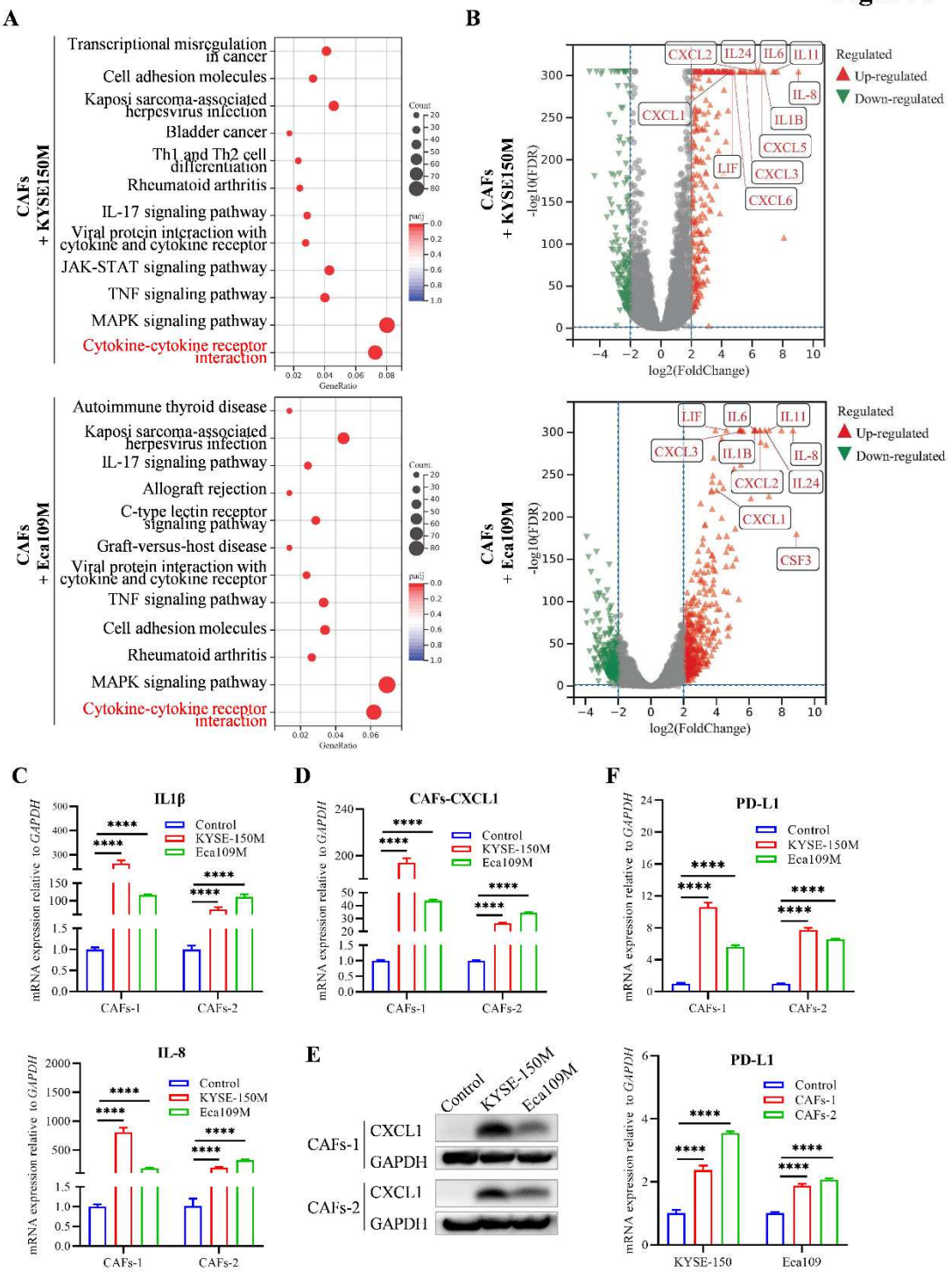


Figure. 8 Up-regulation of CXCL1 in CAFs induced an immunosuppressive tumor microenvironment by activation of cGAS/STING pathway. A. Protein-protein interaction analysis of CXCL1 using the string database. B. The proteins expressions of the components of cGAS-STING pathway in CAFs which

were co-cultured with ESCC cells. KYSE-150M: KYSE-150 medium. Eca109M: Eca109 medium. GAPDH was used as a loading control. C. The proteins expressions of the components of cGAS-STING pathway in CAFs which were transfected with scrambled siRNA (Negative Control, siNC) or CXCL1 siRNA (siCXCL1) before co-culture with ESCC cells. KYSE-150M: KYSE-150 medium. Eca109M: Eca109 medium. GAPDH was used as a loading control. D. qRT-PCR analysis of the expressions of PD-L1, IL1β and IL-8 in CAFs which were pretreated with H-151, an inhibitor of cGAS-STING pathway before co-culture with ESCC cells. KYSE-150M: KYSE-150 medium. Eca109M: Eca109 medium. ****P<0.0001. E. The proteins expressions of the components of cGAS-STING pathway as well as PD-L1, IL1β and IL-8 in CAFs which were pretreated with H-151, an inhibitor of cGAS-STING pathway before co-culture with ESCC cells. KYSE-150M: KYSE-150 medium. Eca109M: Eca109 medium. F. The proteins expressions of PD-L1, IL1β and IL-8 in CAFs which were transfected with scrambled siRNA (Negative Control, NC) or CXCL1 siRNA (siCXCL1) before co-culture with ESCC cells as detected by western blotting analysis. KYSE-150M: KYSE-150 medium. Eca109M: Eca109 medium. GAPDH was used as a loading control. G. The formation of NETs (neutrophil extracellular traps) (indicated by yellow arrows) induced by overexpression of CXCL1 in CAFs as detected by IF analysis. Myeloperoxidase (MPO): a marker of NETs. DAPI was used to visualize the cell nucleus. H. The recruitment of M2 macrophages by overexpression of CXCL1 (CXCL1-OE) in CAFs as detected by transwell assay. **P<0.01. I. The protein expression of CD206, a marker of M2 macrophages, when macrophages were co-cultured with CXCL1-overexpressed (CXCL1-OE) CAFs. GAPDH was used as a loading control.

Figure 8

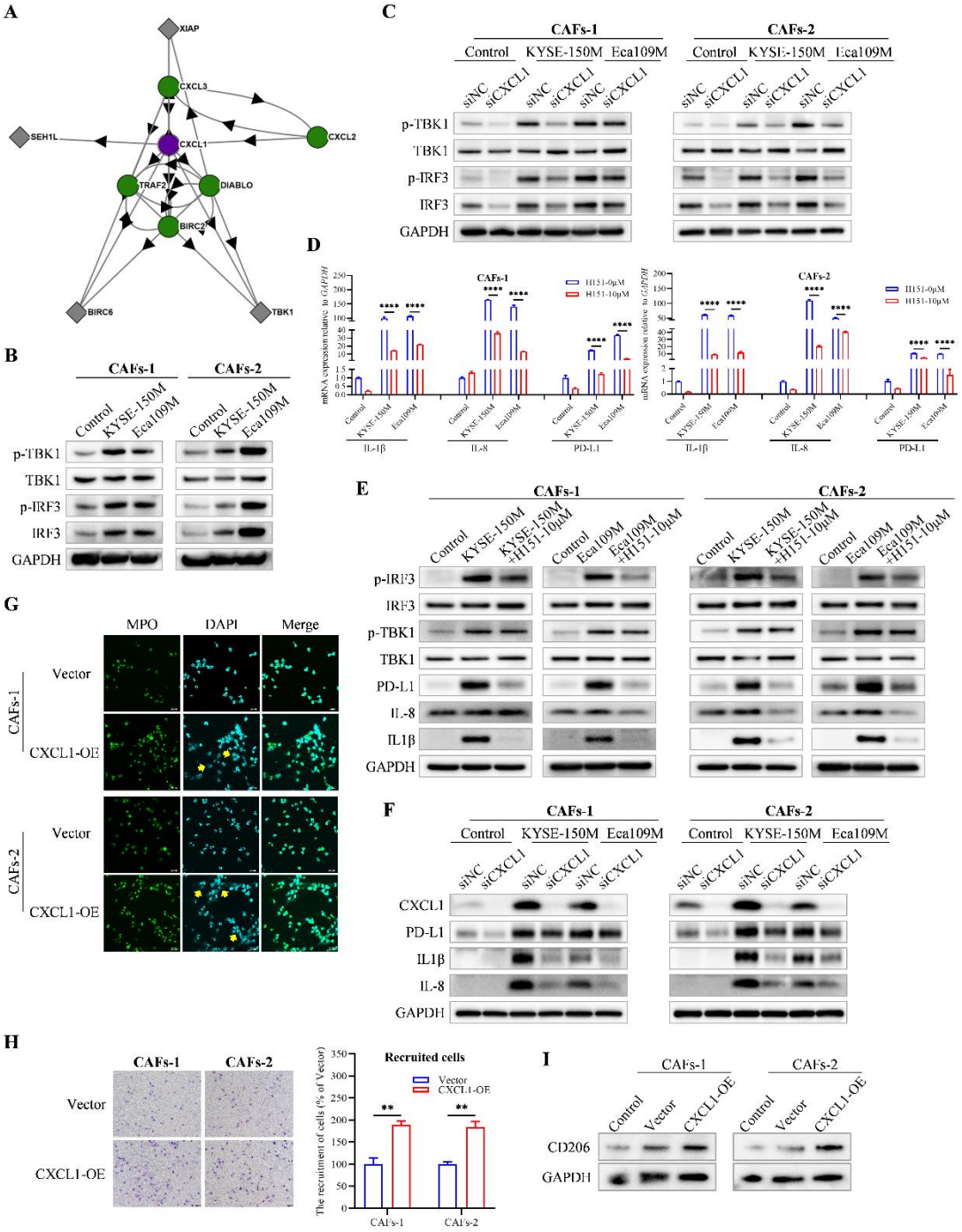


Figure. 9 The schematic diagram of the reciprocal crosstalk between esophageal cancer cells and cancer-associated fibroblasts establishes a pro-metastatic niche by paracrine IGF-2 signaling.

Supplementary Files

This is a list of supplementary files associated with this preprint. Click to download.

- SupportingInformation.doc